Published by Institute of Physics Publishing for SISSA/ISAS
Received: *August 23, 2002*
Revised: *October 5, 2002*
Accepted: *October 15, 2002*

# M-theory on toric $G_2$ cones and its type II reduction

**Lilia Anguelova and Calin I. Lazaroiu**

*C.N. Yang Institute for Theoretical Physics*
*SUNY at Stony Brook NY11794-3840, USA*
*E-mail:* anguelov@insti.physics.sunysb.edu, calin@insti.physics.sunysb.edu

Abstract: We analyze a class of conical $G_2$ metrics admitting two commuting isometries, together with a certain one-parameter family of $G_2$ deformations which preserves these symmetries. Upon using recent results of Calderbank and Pedersen, we extract the IIA reduction of eleven-dimensional supergravity on such backgrounds, as well as its type IIB dual. The associated type II solutions are expected to contain 6-branes and 5-branes respectively. By studying the general asympotics of the IIA and IIB solutions around the relevant loci, we confirm the interpretation of such solutions in terms of localized and delocalized branes. In particular, we find explicit, general expressions for the string coupling and R-R/NS-NS fields in the vicinity of these objects. Our solutions contain and generalize the field configurations relevant for certain models considered in recent work of Acharya and Witten.

Keywords: M-Theory, D-branes, Supergravity Models, Differential and Algebraic Geometry.



http://jhep.sissa.it/archive/papers/jhep102002038/jhep102002038.pdf

JHEP10(2002)038

## Contents





## 1. Introduction

M-theory on backgrounds of $G_2$ holonomy has recently attracted renewed attention [1]–[10]. An interesting class of such models arises from certain non-compact $G_2$ spaces obtained by a construction due to [11] and [12]. These result as cones $\mathcal{C}(Y)$ built over the twistor space $Y$ of a compact, Einstein self-dual space $M$ of positive scalar curvature. In this construction, $Y$ is endowed with a 'twisted' metric, which differs from its canonical Kahler-Einstein metric by certain global and fiberwise rescalings. If one restricts to the case of smooth

$M$, then there are precisely two choices[1] (namely $M = S^4$ and $M = \mathbb{CP}^2$, for which $Y$ is respectively $\mathbb{CP}^3$ and $\mathrm{SU}(3)/\mathrm{U}(1)^2$), both of which were analyzed in [10]. Many more models can be obtained by allowing $M$ to be an orbifold. As pointed out in [8] and [9], such backgrounds are especially interesting from a phenomenological perspective, since their low energy effective description gives four-dimensional, nonabelian gauge theories containing chiral matter. A particular class of such models (namely those based on $M = W\mathbb{CP}^2_{p,q,r}$, endowed with the ESD metrics obtained implicitly in [13]) was analyzed in [9]. For the case when two of weights $p, q, r$ coincide, the authors show that the type IIA reduction leads to configurations of three intersecting D6-branes $B_1, B_2, B_3$, each carrying a nonabelian $\mathrm{SU}(m_j)$ gauge theory, with $m_j$ determined by the weights. The phenomenological relevance of models based on intersecting branes is underscored by the work of [14, 15].

The models considered in [9] share one distinguishing feature. Namely, the ESD metric on $M$ admits a two-torus of isometries, which lift to isometries of the $G_2$ metric on $\mathcal{C}(Y)$ through the construction of [12] and [11]. Therefore, one obtains a natural generalization by allowing $M$ to be an ESD orbifold (compact and of positive scalar curvature) admitting a two-torus of isometries. M-theory on such cones was considered in [16]. There, we presented an algorithm for identifying the type and location of singularities of the $G_2$ cone $\mathcal{C}(Y)$. The work of [16] (which we briefly review in section 2), relies on using a well-known correspondence between ESD spaces and hyperkahler cones [17]–[21]. In the case under consideration, this construction produces a *toric hyperkahler* [22] cone, which can be studied with methods reminiscent of toric geometry [23]–[28]. In [16], we used this observation in order to give general rules for finding the singularities of $\mathcal{C}(M)$, and thus the low energy gauge group of M-theory on such backgrounds. Since the $G_2$ cones considered in [16] admit an isometric $T^2$ action, it is clear that such systems admit T-dual type IIA and type IIB interpretations. By using somewhat abstract arguments, we found that the type IIA reduction of these models will generally contain strongly coupled 6-branes, and that the type IIB description is typically given in terms of (strongly coupled) delocalized 5-branes.

While these results suffice for a qualitative understanding of the physics, one is left wondering about the 11d supergravity and IIA/IIB solutions associated with our models (of which the examples of [9] are a particular case). It turns out that the solutions of interest can be determined explicitly. This follows from a recent result of Calderbank and Pedersen [29], who used an elegant chain of arguments in order to write down the most general ESD metric admitting two independent and commuting Killing fields.[2] For the particular case of positive scalar curvature, they also give the explicit expression of this solution in terms of the toric hyperkahler data which play a central role in [16].

In the present paper, we combine results of [29] and [11, 12] in order to extract the explicit 11d $G_2$ holonomy metric associated with this class of models. Upon reducing through one of the $T^2$ isometries, we will be able to obtain the associated type IIA backgrounds, as

[1] These can be recognized as two of the Wolf-Alekseevskii spaces [37, 38, 39], namely $S^4 = \mathbf{HP}^1 = \mathrm{Sp}(2)/[\mathrm{Sp}(1) \times \mathrm{Sp}(1)]$ and $M = \mathbb{CP}^2 = \mathrm{SU}(3)/\mathrm{U}(2) = Gr_2(\mathbb{C}^3)$, the grassmannian of two planes in $\mathbb{C}^3$. Also note that $\mathbb{CP}^3 = \mathrm{Sp}(2)/[\mathrm{U}(1) \times \mathrm{Sp}(1)]$.

[2] Particular cases of such metrics were considered in [35] and [36].



JHEP10(2002)038

well as their T-dual counterpart in IIB. This gives a discrete infinity of IIA and IIB solutions for certain configurations of localized and delocalized branes which preserve $N = 1$ space-time supersymmetry. Moreover, the asymptotics of the relevant fields around the brane locations provides an independent confirmation of the interpretation proposed in [16].

The present paper is organized as follows. In section 2, we give a brief review of the models of interest and of some basic results of [16]. Section 3 summarizes the result of [29], and explains how it relates to the picture of our previous paper. In section 4, we perform the IIA reduction of the resulting $G_2$ metrics and extract the physical interpretation of the solution by analyzing the asymptotics of various fields around a certain locus. We also explain how this analysis relates to that of [16]. Section 5 considers the T-dual, type IIB solution and its physical interpretation. In section 6, we give a general expression for the calibration 3-form of our models. section 7 presents our conclusions.

## 2. $G_2$ cones from ESD orbifolds.

It is well-known [30, 31] that to every $4d$-dimensional quaternion-Kahler space $M$ one can associate a $4d+2$-dimensional twistor space $Y$ and (modulo the possibility of a double cover) [17, 21, 19, 20, 32] a $4(d+1)$-dimensional hyperkahler cone[3] $X$. This allows one to present the twistor space of $M$ as a Kahler quotient of the hyperkahler cone at some positive moment map level. For $d = 1$, this construction associates an eight-dimensional hyperkahler cone with every compact, ESD space of positive scalar curvature, and reduces the study of its twistor space to that of a certain Kahler quotient of this cone.

On the other hand, the papers [11] and [12] construct a $G_2$ cone from each ESD space of positive curvature.[4] For an ESD space, the twistor space $Y$ can be described as the bundle of unit anti-self-dual two-forms on $M$:

$$Y = B_1(\Lambda^{2,-}(T^*M)) \,. \tag{2.1}$$

This carries the Kahler-Einstein metric:

$$d\rho^2 = |d\sigma|^2 + |d_A\vec{u}|^2 \,, \tag{2.2}$$

where $d\sigma^2$ is the self-dual Einstein metric on $M$, $\vec{u} = (u^1, u^2, u^3)$ are coordinates with respect to a local frame of sections of $\Lambda^{2,-}(T^*M)$ (subject to the constraint $|\vec{u}|^2 = 1$) and the connection $A$ on this bundle is induced by the Levi-Civita connection of $M$.

Following [12, 11], we consider the 'modified' metric on $Y$:

$$d\rho'^2 = \frac{1}{2}\left[d\sigma^2 + \frac{1}{2}|d_A\vec{u}|^2\right] \,, \tag{2.3}$$

and construct a $G_2$ cone $\mathcal{C}(Y)$ as the metric cone over $Y$, taken with respect to this metric:

$$ds^2 = dr^2 + r^2 d\rho'^2 = dr^2 + \frac{r^2}{2}\left(d\sigma^2 + \frac{1}{2}|d_A\vec{u}|^2\right) . \tag{2.4}$$

[3] By definition a hyperkahler cone is a hyperkahler space which can be written as the metric cone over a compact riemannian space.

[4] These papers consider the case when $M$ is smooth, but their results admit an obvious generalization to the orbifold case.

This metric admits a one-parameter family of $G_2$ deformations:

$$ds^2 = \frac{1}{1-(r_0/r)^4}dr^2 + \frac{r^2}{2}\left(d\sigma^2 + \frac{1}{2}\left(1-\left(\frac{r_0}{r}\right)^4\right)|d_A\vec{u}|^2\right), \quad r_0 \geq 0\,, \tag{2.5}$$

with the conical case obtained for $r_0 = 0$.

The papers [10] and [9] studied $M$-theory on such $G_2$ backgrounds for $M$ taken to be $S^4$ or $\mathbb{C}\mathbf{P}^2$ (these are the only smooth choices) and for $M$ given by a weighted projective space, endowed with the orbifold ESD metrics constructed indirectly in [13].

It is now well-established [13, 34, 29, 21, 18] that there exist infinitely many inequivalent Einstein self-dual orbifolds of positive scalar curvature, of which the examples mentioned above form only a small subclass. While the most general model of this type is still beyond reach, there exists a natural class of examples which includes the cases $M = W\mathbb{C}\mathbf{P}^2_{p,q,r}$ while allowing for a wide generalization. This is the class of 'toric' ESD orbifolds, i.e. ESD spaces which possess a two-torus of isometries. As explained in [16], the hyperkahler cone of such a space is 'toric hyperkahler' in the sense of [22],[5] an observation which allows for a systematic analysis of the singularities of its twistor space and associated $G_2$ cone. Moreover, all ESD metrics of this type are known explicitly due to recent work of Calderbank and Pedersen [29].

For such models, the isometries of the four-dimensional base $M$ lift to isometries of the twistor space metrics (2.2) and (2.3). From (2.5), we also find that the latter lift to isometries of the $G_2$ cone and its one parameter deformations. Following [16], $G_2$ isometries of this type will be called *special*. As explained in [16], there exists a correspondence between 'compact' special isometries and vectors of the $\mathbb{Z}^2$ lattice spanned by the toric hyperkahler generators $\nu_j$. M-theory on our $G_2$ backgrounds can be reduced to type IIA upon dividing through a fixed special isometry. This leads to a type IIA background which admits a 'compact' Killing vector field (which generates a U(1) group of isometries), inherited from the two-torus of special isometries upon reduction. This allows one to extract a T-dual type IIB description. It follows that all models of this type admit both IIA and IIB interpretations, namely a pair of such for each choice of special isometry. Before studying these reductions, we review some results of [16] which will help us extract their interpretation.

### 2.1 Eight-dimensional toric hyperkahler cones

As mentioned above, the hyperkahler cones associated with our models are *toric hyperkahler* in the sense of [22]. This means that they are given by torus hyperkahler quotients [33] of the form $X = \mathbf{H}^n///_0\,\mathrm{U}(1)^{n-2}$ of some quaternion affine space $\mathbf{H}^n$ at zero levels of the hyperkahler moment map. The $\mathrm{U}(1)^{n-2}$ action has the following form on affine quaternion coordinates $u_1 \dots u_n \in \mathbf{H}$:

$$u_k \to \prod_{\alpha=1}^{n-2} \lambda_\alpha^{q_k^{(\alpha)}} u_k\,, \tag{2.6}$$

[5] We warn the reader that the terminology 'toric hyperkahler' was used in a different sense in the work of [43, 44, 45]. In this paper, we exclusively use this terminology in the sense of [22].

where $\lambda_\alpha$ are complex numbers of unit modulus and $q_k^{(\alpha)}$ are some integers. The latter form an $(n-2)\times n$ matrix $Q_{\alpha k} = q_k^{(\alpha)}$. To obtain an effective $\mathrm{U}(1)^{n-2}$ action on $\mathbf{H}^n$, one requires that this matrix has unit invariant factors, which amounts to asking that the map of lattices $q^* : \mathbb{Z}^{n-2} \to \mathbb{Z}^n$ associated with the transpose matrix $Q^t$ has torsion-free cokernel. In this case, one obtains a short exact sequence:

$$0 \longrightarrow \mathbb{Z}^{n-2} \xrightarrow{q^*} \mathbb{Z}^n \xrightarrow{g} \mathbb{Z}^2 \longrightarrow 0\,, \tag{2.7}$$

where the map $g$ is represented by a $2\times n$ integral matrix $G$, whose columns $\nu_j = g(e_j) \in \mathbb{Z}^2$ are the so-called *toric hyperkahler generators* (here $e_j$ is the canonical basis of $\mathbb{Z}^n$). The paper [22] focuses on the case of primitive vectors[6] $\nu_j$ and, in fact, considers mostly the case of non-vanishing moment map levels (i.e. studies spaces of the type $X = \mathbf{H}^n///_\xi\, \mathrm{U}(1)^m$ for certain nonzero levels $\xi$). The relevant results of [22] were extended to our situation in the paper [16].

Upon introducing complex coordinates $w_k^{(\pm)}$ through:

$$u_k = w_k^{(+)} + \mathbf{j} w_k^{(-)}\,, \tag{2.8}$$

(where $\mathbf{i},\mathbf{j},\mathbf{k}$ are the imaginary quaternion units, $\mathbf{i}$ being identified with $\sqrt{-1}$), the torus action (2.6) becomes:

$$w_k^{(+)} \to \prod_{\alpha=1}^{n-2} \lambda_\alpha^{q_k^{(\alpha)}} w_k^{(+)}\,, \qquad w_k^{(-)} \to \prod_{\alpha=1}^{n-2} \lambda_\alpha^{-q_k^{(\alpha)}} w_k^{(-)}\,, \tag{2.9}$$

while the $\mathrm{U}(1)$ action leading to the twistor space $Y$ has the form:

$$w_k^{(\pm)} \to \lambda w_k^{(\pm)}\,. \tag{2.10}$$

As in [22], the hyperkahler cone admits a tri-hamiltonian action by the two-torus $\mathrm{U}(1)^2 = \mathrm{U}(1)^n/\,\mathrm{U}(1)^{n-2}$, which allows us to write $X$ as a $T^2$ fibration over $\mathbb{R}^6 = (\mathbb{R}^3)^2$. The fibration map $\vec{\pi} = (\vec{\pi}^{(1)}, \vec{\pi}^{(2)}) : X \to \mathbb{R}^3 \times \mathbb{R}^3$ is the hyperkahler moment map for this $U(1)^2$ action. The fibers of $\vec{\pi}$ can be described explicitly as follows. If one introduces appropriate vector coordinates $\vec{x} = (x_1, x_2, x_3)$ and $\vec{y} = (y_1, y_2, y_3)$ for the two $\mathbb{R}^3$ factors, then the fiber above $(\vec{x}, \vec{y})$ consists of solutions $u = (\{w_k^{(+)}\}, \{w_k^{(-)}\})$ to the system:

$$\frac{1}{2}\left(\left|w_k^{(+)}\right|^2 - \left|w_k^{(-)}\right|^2\right) = \nu_k \cdot a\,, \qquad w_k^{(+)} w_k^{(-)} = \nu_k \cdot b\,, \quad \text{for all } k = 1 \ldots n\,, \tag{2.11}$$

where $a = (x_1, y_1) \in \mathbb{R}^2$ and $b = (x_3 + ix_2, y_3 + iy_2) \in \mathbb{C}^2$. In (2.11), the symbol $\cdot$ stands for the scalar product.

### 2.2 The distinguished locus

It is clear that the singularities of our $G_2$ metrics are immediately known given the singularities of $Y$. The latter were studied in [16] by using the Kahler quotient description $Y = X//_\zeta U(1)$, where $\zeta > 0$ is some level which specifies the overall scale of $Y$ and $\mathrm{U}(1)$

[6] Recall that a vector is called primitive if its components are relatively prime integers.

is the action (2.10). In that paper, we showed that all singularities of the twistor space lie on the so-called *distinguished locus* $Y_D \subset Y$, which is a certain union of holomorphically embedded two-spheres in $Y$. The locus $Y_D$ can be defined abstractly as follows. The $T^2$ fibration $X \to M$ descends to a $T^2$ fibration $Y \to M$ after performing the $U(1)$ Kahler quotient. Then $Y_D$ is the locus in $Y$ where the fibers of this map collapse to a circle or to a point.

The distinguished locus is most easily described in terms of the *characteristic polygon* of $Y$, which is the convex two-dimensional polygon $\Delta$ defined through:

$$\Delta = \left\{ a \in \mathbb{R}^2 \,|\, \sum_{k=1}^{n} |\nu_k \cdot a| = \zeta \right\} . \tag{2.12}$$

This polygon has $2n$ vertices and is symmetric with respect to the reflection $\iota : a \to -a$ through the origin of $\mathbb{R}^2$ (figure 1); its *principal diagonals* (i.e. those diagonals passing through the origin) have the form $D_k := \{a \in \mathbb{R}^2 | \nu_k \cdot a = 0\}$, where $k$ runs from 1 to $n$. In [16], we show that the map $u \to a$ given in (2.11) presents $Y_D$ as an $S^1$ fibration over the one-dimensional space obtained as the union of all edges and principal diagonals of $\Delta$ (see figure 2). The $S^1$ fibers collapse to points above the vertices of the characteristic polygon. This fibration leads to a natural decomposition of the distinguished locus into a *horizontal component* $Y_H$ (the part of $Y_D$ which lies above the edges of $\Delta$) and a *vertical component* $Y_V$ (the part of $Y_D$ lying above the principal diagonals). These further decompose as $Y_H = \cup_{e \in E} Y_e$ and $Y_V = \cup_{k=1}^{n} Y_k$, where $E$ is the set of edges of $\Delta$ and $Y_e$, $Y_j$ are the two-spheres lying above the edge $e$ and above the principal diagonal $D_j$. To describe these two-spheres explicitly, one introduces sign vectors $\epsilon(e) = (\epsilon_1(e) \dots \epsilon_n(e))$ associated with the edges $e$, whose components are defined by:

$$\epsilon_j(e) = \mathrm{sign}(\nu_j \cdot p_e) , \tag{2.13}$$

where $p_e$ is the vector associated with the middle of $e$ (figure 1). Then $Y_e$ is the locus in $Y$ defined by simultaneous vanishing of the complex coordinates $w_1^{(-\epsilon_1(e))} \dots w_n^{(-\epsilon_n(e))}$, while $Y_j$ is defined by vanishing of the quaternion coordinate $u_j$, i.e. by simultaneous vanishing of the complex coordinates $w_j^{(+)}$ and $w_j^{(-)}$. It is also shown in [16] that the spheres $Y_j$ are fibers of the $S^2$ fibration $Y \to M$ (hence the name 'vertical component' for $Y_V$ ) , while $Y_e$ are horizontal with respect to this fibration (i.e. are lifts of spheres lying in the ESD base $M$). The twistor space admits an involution which commutes with the projection $Y \to M$, and thus acts along its $S^2$ fibers. As discussed in [16], the restriction of this 'antipodal map' to the horizontal locus covers the involution $\iota : a \to -a$ of $\Delta$ through the projection map $Y_H \to \Delta$. This implies that the singularity types of $Y$ along $Y_e$ and $Y_{-e}$ coincide, where $e$ and $-e$ are opposite edges of $\Delta$. It also shows that the components $Y_e, Y_{-e}$ of the horizontal locus project to the same locus in the ESD base $M$. The collection of such projections is associated with a polygon $\Delta_M$ on $n$ vertices, obtained as the quotient of $\Delta$ through the sign inversion $\iota$ (figure 1):

$$\Delta_M = \frac{\Delta}{\iota} . \tag{2.14}$$

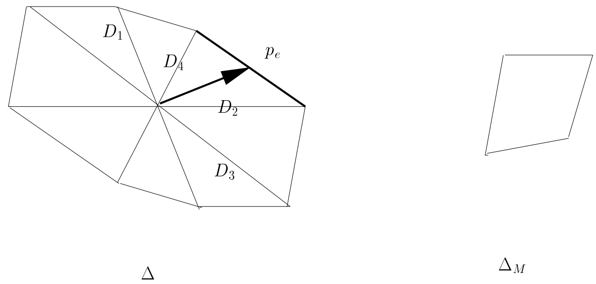


**Figure 1:** Examples of the polygons $\Delta$ and $\Delta_M$ for $n = 4$. For the edge $e$ of $\Delta$ drawn as a bold line, we show the vector $p_e$ used in the definition of the signs $\epsilon_j(e)$. Note that the principal diagonals $D_j = \{a | a \cdot \nu_j = 0\}$ need not lie in trigonometric order.

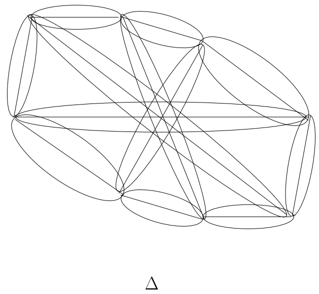


**Figure 2:** Fibration of the distinguished locus over the polygon $\Delta$.

This polygon (which also appeared in the work of [18] and [29], though from a different perspective) will play an important role in what follows.

Assuming that the $\mathbb{Z}_2$ subgroup of $U(1)$ acts nontrivially on $X$ (see (2.10)), it was shown in [16] that $Y$ has a $\mathbb{Z}_{m_e}$ singularity along $Y_e$, where $m_e$ is the greatest common divisor of the two components of the integral vector:

$$\nu_e := \sum_{k=1}^{n} \epsilon_k(e) \nu_k \tag{2.15}$$

(the generic point of $Y_e$ is smooth if $m_e$ equals one). The singularity type along $Y_j$ is given by $\mathbb{Z}_{m_j}$ or $\mathbb{Z}_{2m_j}$, where $m_j$ is the greatest common divisor of the components of the toric hyperkahler generator $\nu_j$. Which of the cases $\mathbb{Z}_{m_j}$ or $\mathbb{Z}_{2m_j}$ occurs along each $Y_j$ can be determined by a simple criterion. These singularity types can be enhanced at the intersection points between $Y_e$ and $Y_j$, which lie above the vertices of $\Delta$. If the $\mathbb{Z}_2$ subgroup of U(1) acts trivially on $X$, then the singularity type along $Y_j$ is always given by $\mathbb{Z}_{m_j}$, while the singularity type along $Y_e$ is 'half' of that determined above (namely in this case $m_e$ is even, and the singularity type is $\mathbb{Z}_{m_e/2}$).

## 3. Toric ESD metrics and $G_2$ metrics

Consider an ESD space $M$ whose associated hyperkahler cone is defined by the exact sequence (2.7). To describe the result of [29], we introduce coordinates $\phi, \psi$ on the $T^2$ fiber of $X \to \mathbb{R}^6$. Recall that a point in $\mathbb{R}^6 = (\mathbb{R}^3)^2$ has the form $(\vec{x}, \vec{y})$, where $\vec{x} = (x_1, x_2, x_3)$

$$
\begin{tikzcd}
X \arrow[r, "\mathbf{H}^*"] \arrow[d, "\vec{\pi}"'] & M \arrow[d, "\pi_M"] \\
\mathbb{R}^6 \arrow[r, "\Theta"'] & \overline{\mathcal{H}}^2
\end{tikzcd}
$$

**Figure 3:** Performing the $\mathbf{H}^*$ quotient.

and $\vec{y} = (y_1, y_2, y_3)$ are real 3-vectors. We denote by $\mathcal{H}^2$ the hyperbolic plane (upper half plane), with coordinates $\eta \in \mathbb{R}$ and $\rho \geq 0$, and by $\overline{\mathcal{H}}^2$ its one-point compactification. The latter is the disk obtained by adding the point $|\eta| = \infty$. Following [29], we define a surjective function $\Theta : \mathbb{R}^3 \times \mathbb{R}^3 \to \overline{\mathcal{H}}^2$ by:

$$\rho = \frac{|\vec{x} \times \vec{y}|^2}{|\vec{x}|^2}, \qquad \eta = \frac{\vec{x} \cdot \vec{y}}{|\vec{x}|^2}. \tag{3.1}$$

It is shown in [29] that the maps in figure 3 form a commutative diagram, whose upper row is the projection $X \to M$ induced by performing a certain $\mathbf{H}^*$ quotient.[7] In fact, the surjection $\pi_M$ on the right presents $M$ as a fibration over the upper half plane, whose generic fiber is a two-torus. The coordinates $\phi, \psi$ descend to coordinates on the $T^2$ fiber of $M$. Hence $(\eta, \rho, \phi, \psi)$ give a coordinate system on $M$, adapted to its $T^2$ fibration over $\overline{\mathcal{H}}^2$.

Let us define a function on $\mathcal{H}^2$ by:

$$F = \sum_{k=1}^{n} \frac{\sqrt{(\nu_k^2)^2\rho^2 + (\nu_k^2\eta + \nu_k^1)^2}}{\sqrt{\rho}}. \tag{3.2}$$

It is then shown in [29] that the Einstein self-dual metric on $M$ has the form:

$$\begin{aligned} d\sigma^2 = {} & \frac{F^2 - 4\rho^2(F_\rho^2 + F_\eta^2)}{4F^2} \, \frac{d\rho^2 + d\eta^2}{\rho^2} + \\ & + \frac{[(F - 2\rho F_\rho)\alpha - 2\rho F_\eta \beta]^2 + [-2\rho F_\eta \alpha + (F + 2\rho F_\rho)\beta]^2}{F^2\left[F^2 - 4\rho^2(F_\rho^2 + F_\eta^2)\right]}, \end{aligned} \tag{3.3}$$

where $\alpha = \sqrt{\rho}\, d\phi$, $\beta = (d\psi + \eta\, d\phi)/\sqrt{\rho}$ and $F_\rho = \partial F/\partial\rho$.

Using topological methods, the authors of [18] prove that the $T^2$ fibers of $M$ collapse to zero size above the boundary $\rho = 0$ of $\overline{\mathcal{H}}^2$. From (3.1), this boundary corresponds to the region of $\mathbb{R}^6$ where $\vec{x}$ and $\vec{y}$ become linearly dependent. At a generic point on $\partial\overline{\mathcal{H}}^2$, one of the cycles of the $T^2$ fiber collapses to a point. The entire two torus collapses to a point at special positions on the boundary [18]. As we shall see in a moment, the boundary $\partial\overline{\mathcal{H}}^2$ can be identified topologically with the polygon $\Delta_M$, in such a way that the vertices of $\Delta_M$ correspond to these special points (figure 4).

[7] The group $\mathbf{H}^* = \mathbf{H}\backslash\{0\}$ has a natural action on the toric hyperkahler cone $X$, induced by the action on $\mathbf{H}^n$ which takes $u_k$ into $u_k t^{-1}$ for all $k = 1, \ldots, n$ (here $t$ is an element of $\mathbf{H}^*$). As reviewed in [16], the $\mathbf{H}^*$ quotient of $X$ recovers the quaternion space $M$. This reduction is a particular case of the so-called 'superconformal quotient' of [40, 41, 42].

JHEP10(2002)038

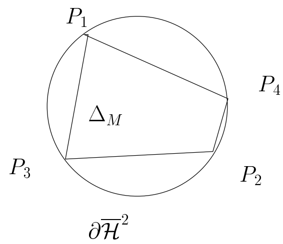


**Figure 4:** The polygon $\Delta_M$ is homeomorphic with the boundary of $\overline{\mathcal{H}}^2$, but not diffeomorphic with it. The figure shows the case $n = 4$.

As recalled above, the $T^2$ fiber of $Y \to M$ collapses along the distinguished locus $Y_D$. The same must obviously be true for the projection of this locus to the self-dual manifold $M$. Hence the distinguished locus projects to a locus $M_D$ in $M$, which sits above the boundary of $\overline{\mathcal{H}}^2$. To understand this projection explicitly, consider first a vertical component $Y_k$, which corresponds to $\nu_k \cdot a = \nu_k \cdot b = 0$ i.e. $\nu_k^1\vec{x} + \nu_k^2\vec{y} = 0$. On this subset of $\mathbb{R}^6$, one has $\rho = 0$ and $\eta = -\nu_k^1/\nu_k^2$, which gives points $P_k$ $(k = 1 \dots n)$ lying on $\partial\overline{\mathcal{H}}^2$. A horizontal component $Y_e$ corresponds to $b = 0 \Leftrightarrow x_2 = x_3 = y_2 = y_3 = 0$ and a certain choice $\epsilon_k(e)$ for the signs of the scalar products $\nu_k \cdot a = \nu_k^1 x_1 + \nu_k^2 y_1$. This gives $\rho = 0$ and a range for the slope $\eta = y_1/x_1$. Therefore, one obtains a segment on $\partial\overline{\mathcal{H}}^2$, connecting two of the points $P_k$. It is also clear that the locus $Y_{-e}$ associated with the opposite edge of $\Delta$ gives the same segment on this boundary. Putting everything together, we find that $\partial\overline{\mathcal{H}}^2$ can be identified with the polygon $\Delta_M$ of the previous subsection, such that the points $P_k$ correspond to its vertices (see figure 4). The $T^2$ fiber of $M$ collapses to a circle above the interior of the edges of $\Delta_M$ and to a point above its vertices. This picture agrees with that of [18]. In this paper, we shall freely use the identification $\Delta_M \equiv \partial\overline{\mathcal{H}}^2$, therefore identifying the edges of $\Delta_M$ with the circular segments $(P_k, P_{k+1})$.

**Observation 1.** Note that the circular segment $(P_k, P_{k+1})$ on the boundary of $\overline{\mathcal{H}}^2$ is characterized by the condition $\rho = 0$ and a choice for the signs $\epsilon_j(\eta) := \mathrm{sign}(\nu_j^2\eta + \nu_j^1)$. Indeed, the quantity $\nu_k^2\eta + \nu_k^1$ changes sign precisely at the point $P_k$ (given by $\eta = \eta_k := -\nu_k^1/\nu_k^2$). Therefore, the signs $\epsilon_j(\eta)$ must be constant on each of the (open) circular segments $(P_k, P_{k+1})$, and the sign vector $\epsilon(\eta) := (\epsilon_1(\eta) \dots \epsilon_n(\eta))$ must have a different value on each such segment. Since $\nu_k \cdot a = \nu_k^1 x_1 + \nu_k^2 y_1 = x_1(\nu_k^2\eta + \nu_k^1)$ for the locus $Y_e$ (remember that $\eta = y_1/x_1$ for such a locus), we have $\epsilon_k(e) = \mathrm{sign}(\nu_k \cdot a) = \mathrm{sign}(x_1)\epsilon_k(\eta)$. The difference between the two edges $e$ and $-e$ of $\Delta$ which lie above an edge $(P_k, P_{k+1})$ of $\Delta_M$ is specified by the sign of $x_1$. In particular, the vector $\nu_e$ of equation (2.15) has the form:

$$\nu_e = \mathrm{sign}(x_1)\nu_\epsilon\,, \tag{3.4}$$

where[8] $\nu_\epsilon := \sum_{k=1}^n \epsilon_k(\eta)\nu_k$. Since $gcd(\nu_e^1, \nu_e^2) = gcd(\nu_\epsilon^1, \nu_\epsilon^2)$, it follows that the singularity type of the twistor space along $Y_e$ and $Y_{-e}$ can also be determined from the vector $\nu_\epsilon$. This observation will be used in sections 4 and 5.

[8] We warn the reader that the notation $\nu_\epsilon$ was used with a different meaning in the paper [16].

**Observation 2.** By using an $\mathrm{SL}(2,\mathbb{Z})$ transformation, one can always arrange that $\nu_j^2$ are non-vanishing for all $j$. In this case, none of the vertices $\eta_j$ of $\Delta_M$ coincide with the compactification point $\eta = \infty$. Throughout this paper, we shall assume that the toric hyperkahler generators satisfy this condition.

**Observation 3.** The coordinates $\psi, \phi$ appearing in (3.3) may have to be subjected to a $\mathbb{Z}_2$ identification. Let us assume for simplicity that the $\mathbb{Z}_2$ subgroup $\{-1, 1\}$ of $\mathbf{H}^*$ acts nontrivially on $X$. Then $\psi, \phi$ are taken to have periodicity $2\pi$. When descending to $M$ via the $\mathbf{H}^*$ quotient, the action of the $\mathbb{Z}_2$ subgroup $\{-1, 1\}$ of $\mathrm{Sp}(1) \subset \mathbf{H}^*$ projects trivially through $\vec{\pi}$, and therefore identifies the $T^2$ fiber of $X$ with itself. This means that $\psi, \phi$ give coordinates on a double cover of the fiber of $M$. Let us consider the degeneration of the latter above an edge $e$ of $\Delta_M$. As explained in [16], this corresponds to the locus $X_e$ in $X$ defined by the equations $w_j^{(-\epsilon_j(e))} = 0$. From the results of [16], we know that the fiber of $X$ is non-degenerate above this locus. However, a certain $\mathrm{U}(1)$ subgroup of $\mathrm{Sp}(1) \subset \mathbf{H}^*$ (given in (2.10)) will act vertically above such an edge. This means that the restriction of $\vec{\pi}$ to $X_e$ is invariant not only under the $\mathbb{Z}_2$ action mentioned above, but under the action of this whole $\mathrm{U}(1)$ subgroup. This is why the fiber of $M$ degenerates to a circle above this edge: the circle is the quotient of the $T^2$ fiber of $X$ through this $\mathrm{U}(1)$ action. Because the $\mathbb{Z}_2$ subgroup lies inside $\mathrm{U}(1)$, the identification mentioned above is automatically implemented by the $\mathrm{U}(1)$ quotient, and the coordinate induced on the $S^1$ fiber of $M$ above $e$ will not be subject to any further discrete quotient. The situation is more complicated above a vertex $\eta_j$ of $\Delta_M$. As explained in [16], the associated locus in $X$ is given by $X_j = \{u \in X | u_j = 0\}$. In this case, the $T^2$ fiber of $X$ collapses to a circle on $X_j$, and the $\mathrm{U}(1)$ subgroup of $\mathrm{Sp}(1)$ does not fix its $\vec{\pi}$-projection — this projection is fixed only by the $\mathbb{Z}_2$ subgroup. If the $\mathbb{Z}_2$ action is nontrivial when restricted to $X_j$, then the fiber of $M$ above the vertex $\eta_j$ is a $\mathbb{Z}_2$ quotient of the $S^1$ fiber of $X$ along $X_j$; this means that the coordinate induced by $\psi, \phi$ along the fiber of $M$ must be subjected to a $\mathbb{Z}_2$ identification. If the $\mathbb{Z}_2$ subgroup acts trivially on $X_j$, then such a further identification does not occur. Which of these cases occurs can be decided by using the criteria of [16]. A similar analysis goes through if the $\mathbb{Z}_2$ subgroup of $\mathrm{Sp}(1)$ acts trivially on $X$, with the conclusion that a further identification must be present above the entire polygon $\Delta_M$. Due to such double cover issues, the gauge group content computed in sections 4 and 5 below may have to be 'halved' in certain situations. In this paper, we shall make the following simplifying assumptions:

(1) First, we require that the $\mathbb{Z}_2$ subgroup of $\mathrm{Sp}(1)$ acts nontrivially on $X$ (a criterion for when this happens can be found in [16]).

(2) We shall further assume that the fibers of $M$ are not subject to any further identifications above the vertices of the polygon $\Delta_M$ (this holds, for example, for the model discussed in [16, section 2]).

These assumptions will allow us to avoid a lengthy case by case analysis and streamline the presentation. The modifications needed in the general case can be easily recovered by using the results of [16].



JHEP10(2002)038

## 4. Reduction to IIA

We are now ready to explore the $G_2$ metric (2.5), where $d\sigma^2$ is given explicitly by (3.3). Remember that the $G_2$ metric admits two commuting U(1) isometries (given by shifts of the coordinates $\phi$ and $\psi$), and that the compact isometries they generate are in correspondence with the two-dimensional lattice spanned by the toric hyperkahler generators $\nu_j$. Hence we can write down the 10-dimensional IIA background obtained by reduction along one of these directions. We can always choose $\phi$ without loss of generality; any other choice (i.e. any primitive, integral linear combination of $\phi$ and $\psi$) can be reduced to this upon performing modular transformations of the lattice spanned by $\nu_1 \dots \nu_n$ (this amounts to changing the integral basis in which these vectors are expressed). With our notations, the coordinates $\psi, \phi$ correspond respectively to the first and second coordinates on $\mathbb{Z}^2$. Therefore, the vector $\nu \in \mathbb{Z}^2$ corresponds to an isometry in the direction $\phi$ if and only if $\nu^1 = 0$.

### 4.1 The reduction

The reduction along $\phi$ results from the standard KK ansatz:

$$ds^2_{(11)} = e^{-(2/3)\varphi_A(x)} g_{\mu\nu}(x) dx^\mu dx^\nu + e^{(4/3)\varphi_A(x)} (d\phi + dx^\mu C_\mu(x))^2 . \tag{4.1}$$

This produces a 10-dimensional IIA bosonic background $(\varphi_A, g_{\mu\nu}, B_{\mu\nu} = 0)$ in the NS-NS sector and $(C_\mu, A_{\mu\nu\rho} = 0)$ in the RR sector. In our case the $B$ field and the three form $A_{\mu\nu\rho}$ vanish because we start with a vacuum configuration in 11 dimensions:

$$ds^2 = ds^2\left(\mathbf{E}^{3,1}\right) + \frac{1}{f} dr^2 + \frac{r^2}{2}\left[d\sigma^2 + \frac{f}{2}|d_A \vec{u}|^2\right] \tag{4.2}$$

and vanishing $11d$ supergravity three-form field. In (4.2) $\mathbf{E}^{3,1}$ is $4d$ Minkowski space and $f(r) = 1 - (r_0/r)^4$.

Upon defining:

$$\begin{aligned}
A(\rho,\eta) &= \frac{F^2 - 4\rho^2(F_\rho^2 + F_\eta^2)}{4F^2\rho^2} \\
B(\rho,\eta) &= \frac{4\left(F_\eta^2 + F_\rho^2\right)\rho^3 - 4\rho^2 F F_\rho + \left[F^2 + 4\eta^2(F_\rho^2 + F_\eta^2) - 8\eta F F_\eta\right]\rho + 4\eta^2 F F_\rho + (\eta^2/\rho)F^2}{F^2\left[F^2 - 4\rho^2(F_\rho^2 + F_\eta^2)\right]}, \\
D(\rho,\eta) &= \frac{4\left(F_\eta^2 + F_\rho^2\right)\rho + 4FF_\rho + (F^2/\rho)}{F^2\left[F^2 - 4\rho^2(F_\rho^2 + F_\eta^2)\right]}, \\
E(\rho,\eta) &= \frac{4\left[-F_\eta F + \eta(F_\eta^2 + F_\rho^2)\right]\rho + 4\eta F F_\rho + (\eta/\rho)F^2}{F^2\left[F^2 - 4\rho^2(F_\rho^2 + F_\eta^2)\right]},
\end{aligned} \tag{4.3}$$

we can write the Einstein self-dual metric on $M$ in the following form:

$$d\sigma^2 = A(d\rho^2 + d\eta^2) + B\, d\phi^2 + D\, d\psi^2 + 2\, E\, d\phi\, d\psi . \tag{4.4}$$

Writing the connection on the bundle $\Lambda^{2,-}(T^*M)$ as $A^j = A^j_\rho(\rho,\eta)d\rho + A^j_\eta(\rho,\eta)d\eta + A^j_\phi(\rho,\eta)d\phi + A^j_\psi(\rho,\eta)d\psi$,[9] $j = 1,2,3$ and $\epsilon^{ijk}A^j u^k$ as $(\vec{A}\times\vec{u})^i$, we can split $|d_A\vec{u}|^2 = (du^i + \epsilon^{ijk}A^j u^k)^2$ into the following terms:

$$|d_A\vec{u}|^2 = H(\vec{u},\rho,\eta) + P_\phi\, d\phi^2 + P_\psi\, d\psi^2 + 2\,P_{\phi\psi}\, d\phi\, d\psi + 2\,Q_\phi\, d\phi + 2\,Q_\psi\, d\psi\,. \tag{4.5}$$

Here:

$$H = \Big[d\vec{u} + (\vec{A}_\rho\times\vec{u})\, d\rho + (\vec{A}_\eta\times\vec{u})\, d\eta\Big]^2 \tag{4.6}$$

is a 2-form independent of $\phi$ and $\psi$ and:

$$\begin{aligned}
P_\phi &= |\vec{A}_\phi\times\vec{u}|^2\\
P_\psi &= |\vec{A}_\psi\times\vec{u}|^2\\
P_{\phi\psi} &= (\vec{A}_\phi\times\vec{u})\,\cdot(\vec{A}_\psi\times\vec{u})\\
Q_\phi &= d\vec{u}\,\cdot\,(\vec{A}_\phi\times\vec{u}) + (\vec{A}_\rho\times\vec{u})\,\cdot(\vec{A}_\phi\times\vec{u})\,d\rho + (\vec{A}_\eta\times\vec{u})\,\cdot(\vec{A}_\phi\times\vec{u})\,d\eta\\
Q_\psi &= d\vec{u}\,\cdot\,(\vec{A}_\psi\times\vec{u}) + (\vec{A}_\rho\times\vec{u})\,\cdot(\vec{A}_\psi\times\vec{u})\,d\rho + (\vec{A}_\eta\times\vec{u})\,\cdot(\vec{A}_\psi\times\vec{u})\,d\eta\,.
\end{aligned} \tag{4.7}$$

Recall that $u^i$ satisfy the constraint $\sum_{i=1}^3 u^i u^i = 1$. The connection $A = A^1\mathbf{i} + A^2\mathbf{j} + A^3\mathbf{k}$ was calculated in [29, section 8]:

$$\begin{aligned}
\vec{A}_\phi &= \left(0, -\frac{\sqrt{\rho}}{F}, \frac{\eta}{F\sqrt{\rho}}\right) \qquad & \vec{A}_\psi &= \left(0,0,\frac{1}{F\sqrt{\rho}}\right)\\
\vec{A}_\rho &= \left(-\frac{F_\eta}{F},0,0\right) & \vec{A}_\eta &= \left(\frac{1}{2\rho}+\frac{F_\rho}{F},0,0\right).
\end{aligned} \tag{4.8}$$

Using this result, we obtain:

$$\begin{aligned}
H =&\ |d\vec{u}|^2 + [1-(u^1)^2]\left[\frac{F_\eta}{F}d\rho - \left(\frac{1}{2\rho}+\frac{F_\rho}{F}\right)d\eta\right]^2 +\\
&+2\left[\frac{F_\eta}{F}d\rho - \left(\frac{1}{2\rho}+\frac{F_\rho}{F}\right)d\eta\right](u^3du^2 - u^2du^3)
\end{aligned}$$

and:

$$\begin{aligned}
P_\phi &= \frac{(u^2\eta+u^3\rho)^2 + (u^1)^2(\rho^2+\eta^2)}{\rho F^2} = \frac{\rho^2+\eta^2-(u^2\rho-u^3\eta)^2}{\rho F^2}\\
P_\psi &= \frac{(u^1)^2+(u^2)^2}{\rho F^2} = \frac{1-(u^3)^2}{\rho F^2}\\
P_{\phi\psi} &= \frac{[(u^1)^2+(u^2)^2]\eta + u^2u^3\rho}{\rho F^2} = \frac{\eta + u^3(u^2\rho - u^3\eta)}{\rho F^2}\\
Q_\phi &= \frac{1}{\sqrt{\rho}F}\Bigg\{u^1(\eta\, du^2 + \rho\, du^3) - (u^2\eta + u^3\rho)\, du^1 +\\
&\qquad + u^1(u^3\eta - u^2\rho)\left[\frac{F_\eta}{F}d\rho - \left(\frac{1}{2\rho}+\frac{F_\rho}{F}\right)d\eta\right]\Bigg\}\\
Q_\psi &= \frac{1}{\sqrt{\rho}F}\left\{u^1du^2 - u^2du^1 + u^1u^3\left[\frac{F_\eta}{F}d\rho - \left(\frac{1}{2\rho}+\frac{F_\rho}{F}\right)d\eta\right]\right\}.
\end{aligned} \tag{4.9}$$

[9]The components of $A$ do not depend on $\phi$ and $\psi$ because the isometries of $M$ lift to isometries of the twistor space, as discussed in section 2 (below eq. (2.5)).

The second equalities in $P_\phi$, $P_\psi$ and $P_{\phi\psi}$ are obtained upon using the constraint $|\vec{u}|^2 = 1$. Let us define a symmetric two by two matrix $U$ with entries:

$$U_{11} = B + \frac{f}{2}P_\phi\,, \qquad U_{22} = D + \frac{f}{2}P_\psi\,, \qquad U_{12} = U_{21} = E + \frac{f}{2}P_{\phi\psi}\,. \tag{4.10}$$

This allows us to write the eleven-dimensional metric (4.2) in the form:

$$ds^2 = ds^2(\mathbf{E}^{3,1}) + \frac{1}{f}dr^2 + \frac{r^2}{2}[U_{11}d\phi^2 + U_{22}d\psi^2 + 2U_{12}d\phi d\psi + 2\bar{Q}_\phi d\phi + 2\bar{Q}_\psi d\psi + \bar{H}]\,, \tag{4.11}$$

where:

$$\bar{H} = \frac{f}{2}H + A\,(d\rho^2 + d\eta^2) \tag{4.12}$$

and

$$\bar{Q}_\phi = \frac{f}{2}Q_\phi\,, \qquad \bar{Q}_\psi = \frac{f}{2}Q_\psi\,. \tag{4.13}$$

To further simplify this expression, we introduce the one-forms:

$$\alpha_1 = \frac{U_{22}\bar{Q}_\phi - U_{12}\bar{Q}_\psi}{\det U}\,, \qquad \alpha_2 = \frac{U_{11}\bar{Q}_\psi - U_{12}\bar{Q}_\phi}{\det U} \tag{4.14}$$

as well as the two-form:

$$\bar{h} = \bar{H} + U_{11}\alpha_1^2 + 2U_{12}\alpha_1\alpha_2 + U_{22}\alpha_2^2\,, \tag{4.15}$$

all of which depend only on $\rho, \eta$ and $\vec{u}$. If we let $\phi_1 \equiv \phi$ and $\phi_2 \equiv \psi$, then the 11d metric becomes:

$$ds^2 = ds^2(\mathbf{E}^{3,1}) + \frac{1}{f}dr^2 + \frac{r^2}{2}[U_{ij}(d\phi_i + \alpha_i)(d\phi_j + \alpha_j) + \bar{h}]\,. \tag{4.16}$$

The virtue of this form of the metric is that it is adapted to the $T^2$ fibration of the ESD base $M$ over the hyperbolic plane $(\rho, \eta)$, which in turn induces a similar fibration of the $G_2$ cone over a five-dimensional space spanned by the coordinates $r, \rho, \eta$ and $\vec{u}$. The entries of the matrix $U$ characterize the metric induced on the $T^2$ fibers.

Recall that we want to perform dimensional reduction along $\phi \equiv \phi_1$. Comparing the last equation with (4.1) we read off the IIA dilaton and RR 1-form:

$$\varphi_A = \frac{3}{4}\ln\left(\frac{r^2U_{11}}{2}\right) \qquad C = \frac{U_{12}d\psi + \bar{Q}_\phi}{U_{11}} = \frac{U_{12}d\psi + \alpha_1 U_{11} + \alpha_2 U_{12}}{U_{11}}\,. \tag{4.17}$$

For the IIA metric in string frame we obtain:

$$\begin{aligned} ds_A^2 = \left(\frac{r^2U_{11}}{2}\right)^{1/2}\Bigg\{ & ds^2(\mathbf{E}^{3,1}) + \frac{1}{f}dr^2 + \frac{r^2}{2U_{11}}[\det U d\psi^2 + 2\,(U_{11}\bar{Q}_\psi - U_{12}\bar{Q}_\phi)d\psi - \\ & - \bar{Q}_\phi^2 + U_{11}\bar{H}]\Bigg\} \end{aligned} \tag{4.18}$$

$$\begin{aligned} = \left(\frac{r^2U_{11}}{2}\right)^{1/2}\Bigg\{ & ds^2(\mathbf{E}^{3,1}) + \frac{1}{f}dr^2 + \frac{r^2}{2U_{11}}[\det U d\psi^2 + 2\det U\alpha_2 d\psi - 2(\alpha_1 U_{11} + \alpha_2 U_{12})^2 - \\ & - \alpha_2^2 \det U + U_{11}\bar{h}]\Bigg\}\,, \end{aligned} \tag{4.19}$$

which in particular gives the components:

$$
\begin{aligned}
g^{(A)}_{\psi\psi} &= \left(\frac{r^2 U_{11}}{2}\right)^{1/2} \frac{r^2 \,\det U}{2\,U_{11}} \\
g^{(A)}_{\psi\rho} &= \left(\frac{r^2 U_{11}}{2}\right)^{1/2} \frac{r^2 f u^1}{4U_{11}F\sqrt{\rho}} \frac{F_\eta}{F}[U_{11}u^3 - U_{12}(u^3\eta - u^2\rho)] \\
g^{(A)}_{\psi\eta} &= -\left(\frac{r^2 U_{11}}{2}\right)^{1/2} \frac{r^2 f u^1}{4U_{11}F\sqrt{\rho}} \left(\frac{1}{2\rho} + \frac{F_\rho}{F}\right)[U_{11}u^3 - U_{12}(u^3\eta - u^2\rho)] \\
g^{(A)}_{\psi u^1} &= \left(\frac{r^2 U_{11}}{2}\right)^{1/2} \frac{r^2 f}{4U_{11}F\sqrt{\rho}} \left[U_{12}\left(u^2\eta + \frac{1-(u^2)^2}{u^3}\rho\right) - U_{11}u^2\right] \\
g^{(A)}_{\psi u^2} &= -\left(\frac{r^2 U_{11}}{2}\right)^{1/2} \frac{r^2 f}{4U_{11}F\sqrt{\rho}} \left[U_{12}\left(u^1\eta - \frac{u^1u^2\rho}{u^3}\right) - U_{11}u^1\right],
\end{aligned}
\tag{4.20}
$$

where we used the relation $du^3 = -(u^1\,du^1 + u^2\,du^2)/u^3$. The remaining $g_{\psi m}$ are zero.

Let us introduce spherical coordinates[10] $\theta, \chi$ through the relations:

$$
u^3 = \cos\theta\,, \qquad u^1 = \sin\theta\cos\chi\,, \qquad u^2 = \sin\theta\sin\chi\,, \tag{4.21}
$$

where $\theta \in [0,\pi]$ and $\chi \in [0, 2\pi]$. One computes:

$$
\begin{aligned}
g^{(A)}_{\psi\chi} &= \left(\frac{r^2 U_{11}}{2}\right)^{1/2} \frac{r^2 f}{4U_{11}F\sqrt{\rho}} \left[U_{11}\sin^2(\theta) - U_{12}\left(\frac{\rho}{2}\sin(2\theta)\sin\chi + \eta\sin^2(\theta)\right)\right] \\
g^{(A)}_{\psi\theta} &= \left(\frac{r^2 U_{11}}{2}\right)^{1/2} \frac{r^2 f}{4U_{11}F} U_{12}\sqrt{\rho}\cos\chi \\
g^{(A)}_{\theta\theta} &= \left(\frac{r^2 U_{11}}{2}\right)^{1/2} \left[\frac{r^2 f}{4} - \frac{r^2 f^2}{8U_{11}\rho F^2}\rho^2\cos^2(\chi)\right] \\
g^{(A)}_{\chi\chi} &= \left(\frac{r^2 U_{11}}{2}\right)^{1/2} \left[\frac{r^2 f}{4}\sin^2(\theta) - \frac{r^2 f^2}{8U_{11}\rho F^2}\sin^2(\theta)(\eta\sin\theta + \rho\cos\theta\sin\chi)^2\right] \\
g^{(A)}_{\chi\theta} &= \left(\frac{r^2 U_{11}}{2}\right)^{1/2} \frac{r^2 f^2}{8U_{11}\rho F^2} 2\rho\sin\theta\cos\chi(\rho\cos\theta\sin\chi + \eta\sin\theta)\,.
\end{aligned}
\tag{4.22}
$$

In these relations, we have isolated the conformal factor $(r^2 U_{11}/2)^{1/2}$ which multiplies the metric (4.18). Since we will be interested in comparing internal sizes with sizes in the Minkowski directions $\mathbf{E}^{3,1}$, it will often be convenient to work with metric components $\tilde{g}_{ij}$ which do not contain this factor:

$$
g_{ij} = \left(\frac{r^2 U_{11}}{2}\right)^{1/2} \tilde{g}_{ij}\,. \tag{4.23}
$$

[10] The reader may wonder why we didn't do this from the beginning. One reason is that the expressions in terms of $u$ are more compact. For some purposes they are more convenient, for others the spherical coordinates are preferable. We note that the most symmetric form of the metric components is attained if one sets $u^1 = \cos\theta$ and $u^2 = \sin\theta\cos\chi$. However it will be more convenient later to use the definitions in (4.21).

All distances computed with respect to $\tilde{g}_{ij}$ will be indicated by a tilde. In particular, we shall be interested in the metric induced by $\tilde{g}_{ij}$ on the $S^2$ fiber of $Y \to M$:

$$d\tilde{s}^2|_{\theta,\chi} = \frac{r^2}{2}\left[\frac{f}{2}|d\vec{u}|^2 - \frac{\bar{Q}_\phi^2}{U_{11}}|_{du^i du^j}\right]. \tag{4.24}$$

Also note that the square radius of the circle spanned by $\psi$ (with respect to the modified metric $\tilde{g}_{ij}$) equals $\tilde{R}_\psi^2 = \tilde{g}_{\psi\psi} = (r^2/2)(\det U/U_{11})$. Finally, we list the nonzero components of the RR one-form, which can be read off from (4.17):

$$\begin{aligned}
C_\psi &= \frac{U_{12}}{U_{11}} \\
C_\rho &= \frac{f(r)\, u^1 F_\eta}{2\, U_{11}\sqrt{\rho}\, F^2}(u^3\eta - u^2\rho) \\
C_\eta &= \frac{f(r)\, u^1}{2\, U_{11}\sqrt{\rho}\, F}(u^2\rho - u^3\eta)\left(\frac{1}{2\rho} + \frac{F_\rho}{F}\right) \\
C_{u^1} &= -\frac{f(r)}{2\, U_{11}\sqrt{\rho}\, F}\left[u^2\eta + u^3\rho + \frac{(u^1)^2\rho}{u^3}\right] \\
C_{u^2} &= \frac{f(r)\, u^1}{2\, U_{11}\sqrt{\rho}\, F}\left[\eta - \frac{u^2\rho}{u^3}\right].
\end{aligned} \tag{4.25}$$

### 4.2 Behavior of the IIA solution for $\rho \to 0$

As we saw above, the singularities of our $G_2$ spaces occur above the boundary $\rho = 0$ of $\overline{\mathcal{H}}^2$. Following [10, 9], we expect that the dimensional reduction will give a type IIA D-brane configuration and that the D-branes will be localized precisely when the reduction is performed through an isometry of the 11-dimensional metric which fixes the singular loci.[11] We will confirm this expectation by a careful study of the asymptotics of the 10-dimensional fields in the limit $\rho \to 0$. Before embarking on the analysis of the horizontal and vertical loci described in subsection 2.2, we need some preparatory calculations of the asymptotics of various expressions.

Following [16], we shall assume that the toric hyperkahler cone $X$ is *good*, which means that any two of the toric hyperkahler generators are linearly independent. This assumption will be made for the remainder of this paper.

From (3.2) one can see that the behavior of $F$ and $F_\eta$ for $\rho \to 0$ is controlled at all orders by the quantities:

$$L_j(\eta) := \sum_{k=1}^{n} \frac{\epsilon_k(\eta)^j (\nu_k^2)^j}{|\nu_k^2\eta + \nu_k^1|^{j-1}} \qquad (j \geq 0)\,, \tag{4.26}$$

where $\epsilon_k(\eta) := \mathrm{sign}(\nu_k^2\eta + \nu_k^1)$. The leading orders have the form:

$$\begin{aligned}
F &= L_0(\eta)\rho^{-1/2} + \frac{1}{2}L_2(\eta)\rho^{3/2} - \frac{1}{8}L_4\rho^{7/2} + O(\rho^{11/2})\,, \\
F_\eta &= L_1\rho^{-1/2} - \frac{1}{2}L_3\rho^{3/2} + \frac{3}{8}L_5\rho^{7/2} + O(\rho^{11/2})\,.
\end{aligned} \tag{4.27}$$

[11] The prototype example of this construction is the relation between the M-theory Kaluza-Klein monopole and the flat type IIA D6-brane [46].

We note that $L_1(\eta)$ coincides with $\frac{d}{d\eta}L_0(\eta)$, and that:

$$L_0=\sum_{k=1}^n|\nu_k^2\eta+\nu_k^1|\,,\qquad L_1=\sum_{k=1}^n\epsilon_k(\eta)\nu_k^2=\nu^2_{\epsilon(\eta)}\,,\qquad L_2=\sum_{k=1}^n\frac{(\nu_k^2)^2}{|\nu_k^2\eta+\nu_k^1|}\,,\tag{4.28}$$

where $\epsilon(\eta)=(\epsilon_1(\eta)\dots\epsilon_n(\eta))$ and $\nu_\epsilon=\sum_{k=1}^n\epsilon_k(\eta)\nu_k$ (See section 3). With our notations, one has:

$$\nu_\epsilon=\begin{bmatrix}T\\ L_1\end{bmatrix}.\tag{4.29}$$

In particular, $T$ and $L_1$ are constant on each edge of $\Delta_M$, but each of them will generally jump when one passes from one edge to another.

Upon noticing that $|\nu_k^2\eta+\nu_k^1|=\epsilon_k(\eta)(\nu_k^2\eta+\nu_k^1)$, we obtain:

$$L_0(\eta)=\sum_{k=1}^n\epsilon_k(\eta)(\nu_k^2\eta+\nu_k^1)=\eta L_1(\eta)+T(\eta)\,,\tag{4.30}$$

with $T(\eta)=\sum_{k=1}^n\epsilon_k(\eta)\nu_k^1=\nu^1_{\epsilon(\eta)}$. Note that $L_0$ is bounded from below by a strictly positive constant depending on the toric hyperkahler generators $\nu_j$,[12] while $L_1$ and $T$ can be positive or negative and are bounded both from below and from above. On the other hand, $L_2$ is strictly positive for finite $\eta$ but vanishes in the limit $\eta\to\pm\infty$. The latter function tends to $+\infty$ at the values $\eta=\eta_j:=-\nu_j^1/\nu_j^2$.

**Observation 1.** In what follows, we shall encounter the quantity $\delta=L_0L_2-L_1^2$. It is important to realize that it is positive. To see this, notice that substituting $\epsilon_j(\eta)=(\nu_j^2\eta+\nu_j^1)/|\nu_j^2\eta+\nu_j^1|$ in the expression for $L_1$ gives:

$$L_1=\eta L_2+S\,,\tag{4.31}$$

where $S=\sum_{j=1}^n(\nu_j^1\nu_j^2)/|\nu_j^2\eta+\nu_j^1|$. Therefore

$$L_0=\eta^2L_2+\eta S+T\,.\tag{4.32}$$

Using the last two relations one obtains:

$$\delta=L_0L_2-L_1^2=L_2(T-\eta S)-S^2\,.\tag{4.33}$$

Upon noticing that $T-\eta S=\sum_{j=1}^n\frac{(\nu_j^1)^2}{|\nu_j^2\eta+\nu_j^1|}$, this leads to the expression:

$$\delta=\left(\sum_{j=1}^n\frac{(\nu_j^1)^2}{|\nu_j^2\eta+\nu_j^1|}\right)\left(\sum_{j=1}^n\frac{(\nu_j^2)^2}{|\nu_j^2\eta+\nu_j^1|}\right)-\left(\sum_{j=1}^n\frac{\nu_j^1\nu_j^2}{|\nu_j^2\eta+\nu_j^1|}\right)^2\,,\tag{4.34}$$

which is non-negative by the Schwartz inequality. It is clear that $\delta$ can be zero only if the two rows $(\nu_1^1\dots\nu_n^1)$ and $(\nu_1^2\dots\nu_n^2)$ of the matrix $G$ (see subsection 2.1) are proportional; this is impossible since $G$ has maximal rank (recall that its columns $\nu_j$ must generate $\mathbb{Z}^2$). We conclude that $\delta$ is strictly positive. Note, however, that $\delta$ tends to zero for $\eta\to\pm\infty$.

[12]Indeed, we have $n\geq 2$ and the vectors $\nu_j$ cannot all be proportional (remember that they have to span $\mathbb{R}^2$). This shows that $L_0(\eta)$ is strictly positive on the real axis. The statement then follows by continuity of $L_0$ together with the fact that $L_0(\eta)$ tends to $+\infty$ for $\eta\to\pm\infty$. The lower bound is given by $min_{\eta\in\mathbb{R}}L_0(\eta)>0$, which is attained for some value of $\eta$.

**Observation 2.** The quantities $T$ and $\eta_j$ obey certain properties which will be used below. First, notice that $T(0) = \sum_{k=1}^n \mathrm{sign}(\nu_k^1)\nu_k^1 = \sum_{k=1}^n |\nu_k^1|$. Thus vanishing of $T(0)$ would require that all $\nu_k^1$ vanish, which is impossible since they must generate $\mathbb{Z}^2$. It follows that $T(0)$ cannot vanish. If $T$ vanishes along a given edge of $\Delta$, this clearly implies that $\eta = 0$ cannot be an endpoint of this edge. Now suppose that we are given a model for which $\eta = 0$ is a vertex of $\Delta_M$. Then the previous observation shows that $T$ must be non-vanishing along the two edges of $\Delta_M$ which share this vertex. We also note that at most one of the toric hyperkahler generators can have the property $\nu_j^1 = 0$. Indeed, if $\nu_j^1 = \nu_k^1 = 0$ for some $j \neq k$, then the generators $\nu_j$ and $\nu_k$ must be proportional, which contradicts the assumption that the toric hyperkahler cone $X$ is good. As discussed in [16], the requirement that $X$ is good means that the principal diagonals of $\Delta$ cannot coincide, which means that $\Delta$ has $2n$ distinct vertices. This obviously implies that $\Delta_M$ must have $n$ (distinct) vertices, which is another explanation for our second observation above. We shall often use these basic properties in the analysis of sections 4 and 5.

#### 4.2.1 Asymptotics of $U$

Using (4.27), one finds the following expansions for $\rho \to 0$:

$$\begin{aligned}
A &= \frac{\delta}{L_0^2} + O(\rho^2)\,, & B &= \frac{T^2}{L_0^2\delta} + O(\rho^2) \\
D &= \frac{L_1^2}{L_0^2\delta} + O(\rho^2)\,, & E &= -\frac{L_1 T}{L_0^2\delta} + O(\rho^2)
\end{aligned} \tag{4.35}$$

as well as:

$$\begin{aligned}
U_{11} &= \frac{T^2}{L_0^2\delta} + \frac{f}{2}\frac{\eta^2}{L_0^2}\sin^2(\theta) + O(\rho) \\
U_{22} &= \frac{L_1^2}{L_0^2\delta} + \frac{f}{2}\frac{1}{L_0^2}\sin^2(\theta) + O(\rho^2) \\
U_{12} &= -\frac{L_1 T}{L_0^2\delta} + \frac{f}{2}\frac{\eta}{L_0^2}\sin^2(\theta) + O(\rho)\,.
\end{aligned} \tag{4.36}$$

To arrive at the last equations, we used the coordinate transformation (4.21) and the leading asymptotics of the connection (4.8):

$$\begin{aligned}
\vec{A}_\rho &= \left(-\frac{L_1}{L_0}, 0, 0\right) + O(\rho^2)\,, & \vec{A}_\psi &= \left(0, 0, \frac{1}{L_0}\right) + O(\rho^2) \\
\vec{A}_\phi &= \left(0, 0, \frac{\eta}{L_0}\right) + O(\rho)\,, & \vec{A}_\eta &= \rho\left(\frac{L_2}{L_0}, 0, 0\right) + O(\rho^3)\,.
\end{aligned} \tag{4.37}$$

We shall also need the asymptotics of $\det U$. Upon using the higher order asymptotics of $\vec{A}$ and $B, D, E$, one finds:

$$\det U = \frac{f}{2L_0^2}\frac{\sin^2(\theta)}{\delta} + \frac{fL_1}{2L_0^3}\frac{\sin(2\theta)\sin\chi}{\delta}\rho + \frac{\Lambda}{4L_0^4\delta^2}\rho^2 + O(\rho^3)\,, \tag{4.38}$$

where:

$$\Lambda = f\delta(f\delta + 2L_1^2)\sin^2(\theta)\cos^2(\chi) + fL_0\left[L_2(5\delta - L_1^2) + L_0(2L_1L_3 - L_0L_4)\right]\cos^2(\theta) + \\ + 4\delta^2 + f\left[L_0^2(L_0L_4 + L_2^2 - 2L_1L_3) - 2\delta(5\delta + L_1^2)\right] , \tag{4.39}$$

with $\delta = L_0L_2 - L_2^1$ as above.

### 4.2.2 Asymptotics for the metric components along $\psi, \theta$ and $\chi$

Consider the asymptotics of the angular metric components in the coordinates $\theta$, $\chi$ and $\psi$:

$$\begin{aligned}
\tilde{g}^{(A)}_{\theta\theta} &= \frac{r^2 f}{4} + O(\rho^2) \\
\tilde{g}^{(A)}_{\theta\chi} &= O(\rho) \\
\tilde{g}^{(A)}_{\chi\chi} &= \frac{r^2 f}{4}\frac{2T^2\sin^2(\theta)}{2T^2 + f\eta^2\delta\sin^2(\theta)} + O(\rho) \\
\tilde{g}^{(A)}_{\psi\chi} &= \frac{r^2 f}{4}\frac{2T\sin^2(\theta)}{2T^2 + f\eta^2\delta\sin^2(\theta)} + O(\rho) \\
\tilde{g}^{(A)}_{\psi\theta} &= O(\rho) \\
\tilde{g}^{(A)}_{\psi\psi} &= \frac{r^2 f}{4}\frac{2\sin^2(\theta)}{2T^2 + f\eta^2\delta\sin^2(\theta)} + O(\rho) .
\end{aligned} \tag{4.40}$$

The metric (4.24) induced on the $S^2$ fiber takes the following form in the limit $\rho \to 0$:

$$d\tilde{s}^2|_{\theta,\chi} = \frac{r^2 f}{4}\{d\theta^2 + \mathcal{U}(r,\eta,\theta)\sin^2(\theta)d\chi^2\} + O(\rho) . \tag{4.41}$$

The squashing factor $\mathcal{U}$ is given by:

$$\mathcal{U}(r,\eta,\theta) = \frac{2T^2}{2T^2 + f\eta^2\delta\sin^2(\theta)} + O(\rho) . \tag{4.42}$$

However (4.40) shows something more interesting, namely that the metric induced in the directions $\theta, \psi$ and $\chi$ reduces to:

$$d\tilde{s}^2|_{\theta,\chi,\psi} = \frac{r^2 f}{4}\left[d\theta^2 + \frac{2\sin^2(\theta)}{2T^2 + f\eta^2\delta\sin^2(\theta)}(T(\eta)d\chi + d\psi)^2\right] + O(\rho) . \tag{4.43}$$

At a fixed value of $\eta$, this shows that only one of the two periodic directions spanned by $\chi$ and $\psi$ has finite size in the limit $\rho \to 0$. Above a fixed edge of $\Delta_M$, one has $T = \nu^1_\epsilon$, and (4.43) shows that the two-torus spanned by $\chi$ and $\psi$ collapses to the cycle spanned by $\nu^1_\epsilon\chi + \psi$. To make this precise, consider the change of coordinates[13]:

$$\xi = T\chi + \psi , \qquad \zeta = \chi \Longleftrightarrow \psi = \xi - T\zeta , \qquad \chi = \zeta . \tag{4.44}$$

[13] We shall see in a moment that $\xi$ is a good coordinate in a whole tubular neighborhood of the locus $\rho = 0$.



JHEP10(2002)038

The two-torus spanned by $\chi$ and $\psi$ can be viewed as the quotient of $\mathbb{R}^2$ through the integral lattice generated by the tangent vectors $\partial_\chi$ and $\partial_\psi$. The transformation $(\psi,\chi) \to (\xi,\zeta)$ corresponds to an invertible integral transformation implemented by the modular matrix $S = \left[\begin{smallmatrix} 1 & 0 \\ -T & 1 \end{smallmatrix}\right] \in \mathrm{SL}(2,\mathbb{Z})$:

$$\begin{bmatrix} \partial_\xi \\ \partial_\zeta \end{bmatrix} = S \begin{bmatrix} \partial_\psi \\ \partial_\chi \end{bmatrix}, \tag{4.45}$$

i.e.:

$$\partial_\xi = \partial_\psi \,, \qquad \partial_\zeta = \partial_\chi - T\partial_\psi \Longleftrightarrow \partial_\psi = \partial_\xi \,, \qquad \partial_\chi = T\partial_\xi + \partial_\zeta \,. \tag{4.46}$$

Since (4.45) preserves the lattice generated by $\partial_\chi$ and $\partial_\psi$, we obtain new coordinates on this torus upon taking $\xi, \zeta$ to belong to $[0, 2\pi]$. We have:

$$d\xi = Td\chi + d\psi \,, \qquad d\zeta = d\chi \Longleftrightarrow d\psi = d\xi - Td\zeta \,, \qquad d\chi = d\zeta \,. \tag{4.47}$$

The induced metric (4.43) becomes:

$$d\tilde{s}^2|_{\theta,\chi,\psi} = d\tilde{s}^2|_{\theta,\zeta} = \frac{r^2 f}{4}\left[d\theta^2 + \frac{2\sin^2(\theta)}{2T^2 + f\eta^2\delta\sin^2(\theta)} d\xi^2\right] + O(\rho)\,. \tag{4.48}$$

In particular, one has:

$$\begin{aligned} \tilde{R}_\xi^2 &= ||\partial_\xi||^2 = \frac{r^2 f}{4}\frac{2\sin^2(\theta)}{2T^2 + f\eta^2\delta\sin^2(\theta)} + O(\rho)\,, \\ \tilde{R}_\zeta^2 &= ||\partial_\zeta||^2 = O(\rho) \\ \partial_\xi \cdot \partial_\zeta &= O(\rho)\,. \end{aligned} \tag{4.49}$$

Hence the $\xi$- and $\zeta$-cycles become orthogonal for small $\rho$, while the $\zeta$-cycle collapses to zero size (figure 5). In this limit, the $\chi$-cycle becomes a $T$-fold cover of the $\xi$-cycle (figure 6).

To understand the global situation above the polygon $\Delta_M$, consider the behavior of (4.43) near a vertex $\eta = \eta_j := -\nu_j^1/\nu_j^2$. Since $L_0$ remains strictly positive while $L_2(\eta)$ tends to infinity like $1/|\eta - \eta_j|$ for $\eta \to \eta_j$, the behavior of the quantity $\eta^2\delta$ in this limit depends on whether $\eta_j$ is nonzero or not, i.e. $\nu_j^1 \neq 0$ or $\nu_j^1 = 0$. If $\nu_j^1 \neq 0$, we have $\eta^2\delta \to \infty$ and the second term in (4.43) vanishes. This shows that (4.43) is continuous when $\eta$ passes through the value $\eta_j$ at $\rho = 0$. If $\nu_j^1 = 0$, then $\eta^2\delta$ tends to zero for $\eta \to \eta_j = 0$. On the other hand, vanishing of $\nu_j^1$ shows that the quantity $T(\eta) = \nu^1_{\epsilon(\eta)}$ reduces to $\sum_{k\neq j}\epsilon_k(\eta)\nu_k^1$, which has the same value on the two edges of $\Delta_M$ adjacent to the vertex $\eta_j$. Therefore, the coefficients of the induced metric (4.43) are still continuous at $\eta = \eta_j$, where the metric takes the form:

$$d\tilde{s}^2|_{\theta,\chi,\psi} = \frac{r^2 f}{4}\left[d\theta^2 + \frac{\sin^2(\theta)}{T^2}(Td\chi + d\psi)^2\right] + O(\rho\,. \tag{4.50}$$

This shows that there exists a good coordinate $\xi$, defined on a tubular neighborhood of the locus $\rho = 0$, such that $\xi = T(\eta)\chi + \psi + O(\rho)$ for $\rho \to 0$. This allows us to write (4.43) in the form (4.48) with respect to this coordinate.

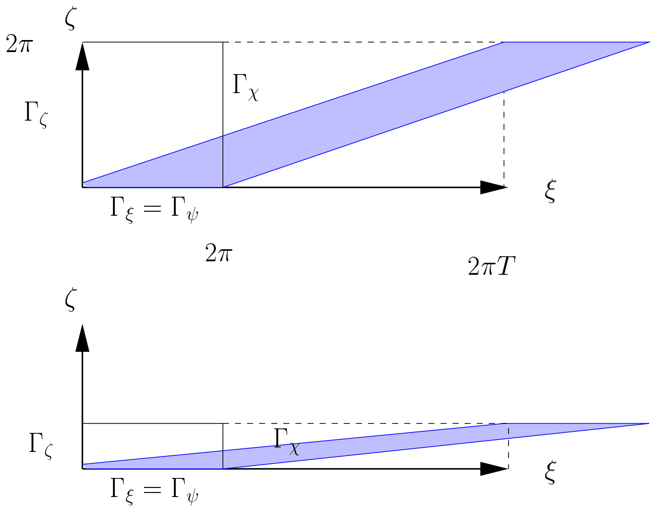


**Figure 5:** The two-torus spanned by $\psi$ and $\chi$. The upper figure is purely topological and shows two elementary cells in the associated integral lattice (whose generators are normalized to have length $2\pi$), for the case $T > 0$. The filled-in cell corresponds to the cycles $\Gamma_\psi$ and $\Gamma_\chi$ (defined respectively by $\chi = 0$ and $\psi = 0$), while the rectangular cell on the left corresponds to $\Gamma_\xi$ and $\Gamma_\zeta$ (defined respectively by $\zeta = 0$ and $\xi = 0$). Taking both $(\psi, \chi)$ and $(\xi, \zeta)$ to belong to $[0, 2\pi]^2$ gives good parameterizations of the same torus. The lower figure shows the metric geometry as $\rho$ approaches zero. In this limit, the length of $\Gamma_\zeta$ tends to zero, so that $\Gamma_\chi$ becomes a $T$-fold cover of $\Gamma_\xi$ (figure 6).

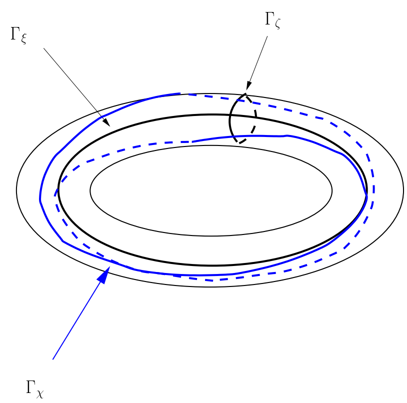


**Figure 6:** The cycle $\Gamma_\chi$ for the case $T = 2$.

Because the $\zeta$-cycle is always collapsed in our limit, the locus $\rho = 0$ has codimension *two*. Fixing the radial coordinate $r$, this locus is described by a fibration over the edges of $\Delta_M$. If $T = \nu^1_\epsilon$ vanishes along some edge, then the induced metric (4.48) reduces to:

$$d\tilde{s}^2|_{\theta,\chi,\psi} = \frac{r^2 f}{4}\left[d\theta^2 + \frac{2}{f\eta^2\delta}d\xi^2\right]. \tag{4.51}$$

Hence the $S^2$ fibers reduce to cylinders of (relative) height $\pi r\sqrt{f}/2$ and radius $r/(|\eta|\sqrt{2\delta})$. The cylinder's radius collapses to zero when $\eta$ approaches the endpoints of this edge (none of which can lie at $\eta = 0$). Therefore, the whole locus sitting above this edge at $\rho = 0$ is a cylinder whose cross section is a two-sphere obtained by fibering the $\xi$-circle above this edge (the radius of the $\xi$-circle collapses above the endpoints). Also note that $\xi = \psi$ along this locus, so that the $\xi$ and $\psi$ circles coincide.

Above a vertex $\eta_j \neq 0$ (so that $\nu_j^1 \neq 0$ and $\eta^2\delta \to \infty$), the induced metric takes the form:

$$d\tilde{s}^2|_{\theta,\chi,\psi} = \frac{r^2 f}{4} d\theta^2 \,, \tag{4.52}$$

and the fiber reduces to a segment of (relative) length $\pi r\sqrt{f}/2$. If one of the toric hyperkahler generators has the property $\nu_j^1 = 0$, then $\eta = 0$ is a vertex of $\Delta_M$ above which (4.48) reduces to the metric (4.50):

$$d\tilde{s}^2|_{\theta,\chi,\psi} = \frac{r^2 f}{4}\left[d\theta^2 + \frac{\sin^2(\theta)}{T^2} d\xi^2\right] . \tag{4.53}$$

Above the interior of an edge having $T \neq 0$, the fiber has topology $S^2$. The behavior at the edge's endpoints depends on whether $\eta$ vanishes there. If $\eta$ does not vanish at the endpoint, then the fiber collapses to a segment (4.52). If $\eta$ vanishes there, then the fiber reduces to the metric (4.53). Figure 7 illustrates this behavior for a particular example in the case $n = 3$.

### 4.2.3 Asymptotics of the coupling constant and RR one-form

It is easy to check that the coupling constant has the behavior:

$$g_A^{4/3} = \frac{r^2 U_{11}}{2} = \frac{r^2}{4}\frac{2T^2 + f\eta^2\delta\sin^2(\theta)}{L_0^2\delta} + O(\rho) \,. \tag{4.54}$$

For the RR one-form, we obtain:

$$\begin{aligned}
C_\psi &= \frac{f\eta\delta\sin^2(\theta) - 2TL_1}{2T^2 + f\eta^2\delta\sin^2(\theta)} + O(\rho) \\
C_\rho &= \frac{f\eta L_1\delta\sin\theta\cos\theta\cos\chi}{2T^2 + f\eta^2\delta\sin^2(\theta)} + O(\rho) \\
C_\eta &= O(\rho) \\
C_{u^1} &= -\frac{f\eta L_0\delta\sin\theta\sin\chi}{2T^2 + f\eta^2\delta\sin^2(\theta)} + O(\rho) \\
C_{u^2} &= \frac{f\eta L_0\delta\sin\theta\cos\chi}{2T^2 + f\eta^2\delta\sin^2(\theta)} + O(\rho) \,.
\end{aligned} \tag{4.55}$$

Upon converting to spherical coordinates on the $S^2$ fibers spanned by $\vec{u}$, one obtains:

$$C = \frac{f\eta\delta\sin^2(\theta) - 2TL_1}{2T^2 + f\eta^2\delta\sin^2(\theta)} d\psi + \frac{f\eta L_1\delta\sin\theta\cos\theta\cos\chi}{2T^2 + f\eta^2\delta\sin^2(\theta)} d\rho + \frac{f\eta L_0\delta\sin^2(\theta)}{2T^2 + f\eta^2\delta\sin^2(\theta)} d\chi + O(\rho) \,, \tag{4.56}$$

where $\delta = L_0 L_2 - L_1^2$. Changing to the coordinates $\xi, \zeta$ gives:

$$C = \frac{f\eta\delta\sin^2(\theta) - 2TL_1}{2T^2 + f\eta^2\delta\sin^2(\theta)} d\xi + \frac{f\eta L_1\delta\sin\theta\cos\theta\cos\zeta}{2T^2 + f\eta^2\delta\sin^2(\theta)} d\rho + L_1 d\zeta + O(\rho) \,, \tag{4.57}$$

where we used the relation $L_0 = \eta L_1 + T$.

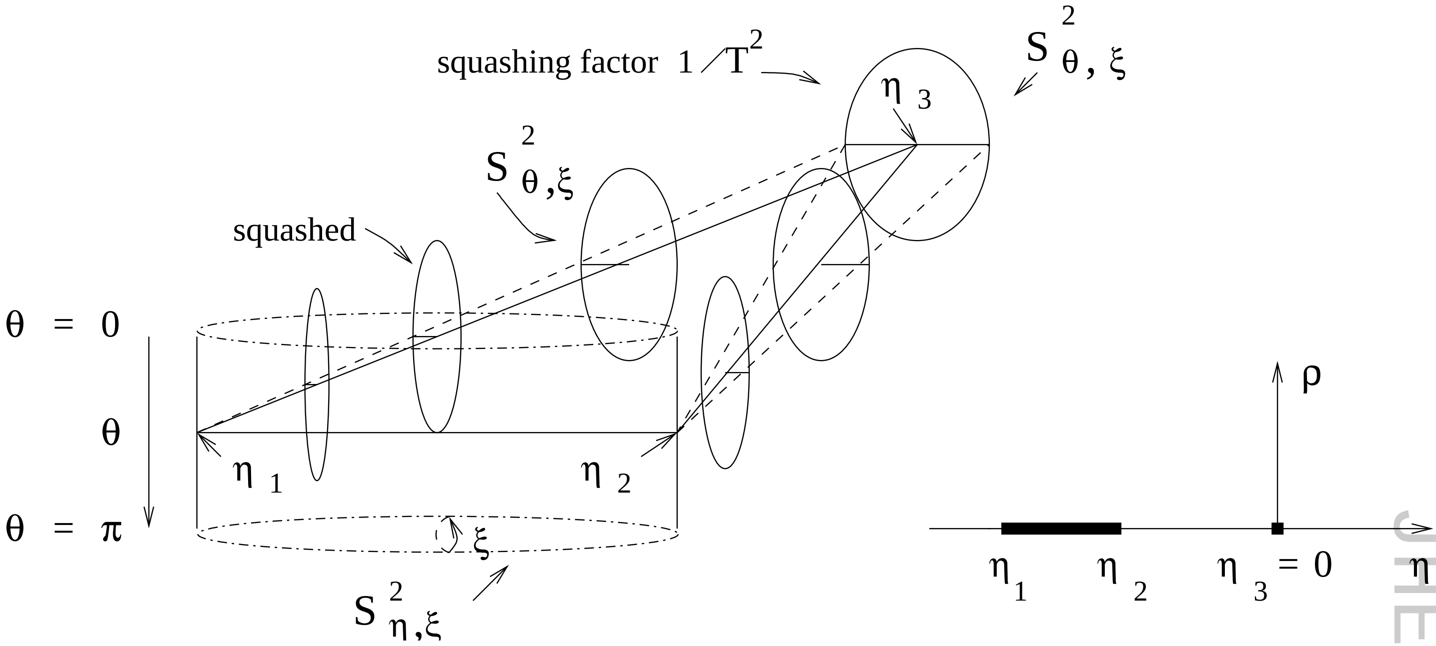


**Figure 7:** The locus $\rho = 0$ at a fixed value of $r$. The figure shows the case $n = 3$, for a model admitting a good isometry. In this case, $\Delta_M$ is a triangle with vertices $\eta_1, \eta_2, \eta_3 \in \partial\overline{\mathcal{H}}^2 = \mathbb{R} \cup \{\infty\}$: these values are displayed on the right. We assume that one reduces to IIA by the good isometry, and that $\nu^1_\epsilon = 0$ along the edge $[\eta_1, \eta_2]$ and $\nu^1_3 = 0$ for the vertex $\eta_3$ (these conditions are satisfied for the models of [9], with an appropriate choice of basis for the lattice spanned by the toric hyperkahler generators). One obtains a three-dimensional cylinder with spherical section sitting above the edge $[\eta_1, \eta_2]$ and a squashed sphere sitting above the vertex $\eta_3$. The two generators of the cylinder sitting above the vertices $\eta_1$ and $\eta_2$ are connected with the sphere which sits above $\eta_3$ by three-dimensional bodies whose generic sections are squashed two-spheres.

Fixing $r, \eta, \theta, \rho$ and $\xi$, one can integrate $C$ over the collapsing $\zeta$-circle $\Gamma_\zeta$ with the result:

$$\int_{\Gamma_\zeta} C = C_\zeta \int_0^{2\pi} d\zeta = 2\pi L_1 + O(\rho) = 2\pi \nu^2_\epsilon + O(\rho)\,. \tag{4.58}$$

In this relation, we assume that $\rho$ is taken to be very small but non-vanishing, so that the cycle $\Gamma_\zeta$ has radius of order $\rho$. This ensures that the asymptotic form (4.57) can be used in (4.58). Integrating over a similar $\xi$-circle (at $\rho$ small but non-zero) gives:

$$\int_{\Gamma_\xi} C = C_\xi \int_0^{2\pi} d\xi = 2\pi \frac{f\eta\delta \sin^2(\theta) - 2TL_1}{2T^2 + f\eta^2\delta \sin^2(\theta)} + O(\rho)\,. \tag{4.59}$$

This shows the existence of flux on the locus $\rho = 0$.

### 4.3 Behavior on the horizontal locus

We are now ready to study the behavior of the type IIA fields (4.17) and (4.18) on the horizontal locus of subsection 2.2. This locus corresponds to $\rho = 0$ and $P_\phi = |\vec{A}_\phi \times \vec{u}|^2 = 0$,[14] at some fixed value of $r$. By virtue of the asymptotic expansion of $\vec{A}_\phi$ given in (4.37) and

[14] As well as $P_\psi = 0$ and $P_{\phi\psi} = 0$. These two equations give the same condition as $P_\phi = 0$ in the limit

the constraint $|\vec{u}| = 1$, the second condition amounts to $\vec{u} = (0, 0, 1)$, which due to (4.21) is equivalent with $\theta = 0, \pi$. These two values of $\theta$ correspond to the two opposite edges of the characteristic polygon $\Delta$ lying above a given edge of $\Delta_M$ (see section 3). Along this locus, the quantities $U_{ij}$ coincide with $B, D, E$.

From expression (4.38), one finds:[15]

$$\det(U) = \frac{1}{L_0^4}\left[1 + \frac{fL_1^2}{2\delta}\right]\rho^2 + O(\rho^3) \quad \text{for} \quad \theta = 0, \pi\,. \tag{4.60}$$

Equation (4.54) gives the behavior of the coupling constant:

$$g_A^{4/3} = \frac{r^2}{2}\frac{T^2}{L_0^2\delta} + O(\rho) \quad \text{for} \quad \theta = 0, \pi\,. \tag{4.61}$$

Let us fix an edge $c$ of $\Delta_M$, and thereby (as explained in section 3) the value of the sign vector $\epsilon$. We let $e$ and $-e$ be the two edges of $\Delta$ lying above $c$, which correspond respectively to the loci $\theta = 0$ and $\theta = \pi$ at $\rho = 0$ and fixed $r$. We obtain the following two cases:

(a) If the edge $c$ satisfies $T = \nu^1_{\epsilon(\eta)} \neq 0$, then equation (4.48) shows that the $(\theta, \zeta)$- fibers above $c$ are squashed two-spheres (figure 8). Further imposing the conditions $\theta = 0, \pi$ gives two segments lying above the edge $c$. Relation (4.57) gives:

$$C = -\frac{L_1}{T}d\xi + L_1 d\zeta + O(\rho) \quad \text{for} \quad \theta = 0, \pi\,, \tag{4.62}$$

while (4.58) becomes:

$$\int_{\Gamma_\zeta} C = 2\pi\nu_\epsilon^2 + O(\rho) \quad \text{for} \quad \theta = 0, \pi\,. \tag{4.63}$$

This shows the existence of $L_1 = \nu_\epsilon^2$ units of flux passing through the poles of each $\theta, \xi$-sphere lying at $\rho = 0$. Equation (4.61) shows that the coupling constant tends to a finite value on this piece of the horizontal locus, which therefore does not admit a perturbative interpretation in IIA string theory.

(b) If $T = \nu^1_\epsilon$ vanishes, then (4.35) gives $B = E = 0$ for $\rho \to 0$. Equation (4.51) shows that the $(\theta, \xi)$ fibers degenerate to two-dimensional cylinders in this limit. As explained above, the part of the locus $\rho = 0$ which sits above the edge $c$ is a three-dimensional cylinder of finite height whose cross section is a two-sphere spanned by $\eta$ and $\xi$. The sublocus $\theta = 0, \pi$ consists of the two spherical ends of this cylinder (figure 9).

Relation (4.54) shows that the type IIA coupling constant vanishes on these ends:

$$g_A^{4/3} = \frac{r^2 f\eta^2}{4L_0^2}\sin^2(\theta) + O(\rho)\,. \tag{4.64}$$

$\rho \to 0$, as is clear from (4.9). The vanishing of those three metric coefficients is an obvious consequence of the fact that the horizontal locus consists of two-spheres lying in the base $M$ (see subsection 2.2).

[15]Indeed, the terms of order $\rho^0$ and $\rho$ vanish while $\Lambda$ reduces to $2(2\delta + fL_1^2)$.

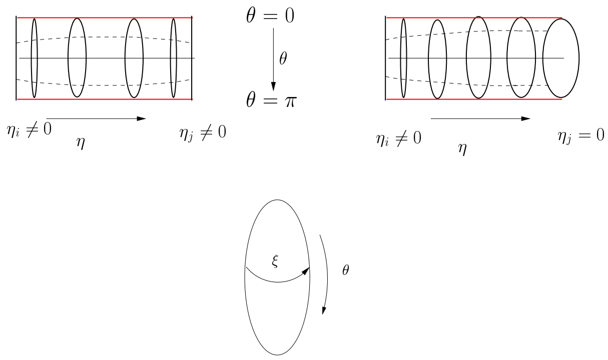


**Figure 8:** The locus $\theta = 0, \pi$ at $\rho = 0$ and fixed $r$ for an edge of $\Delta_M$ which satisfies $\nu^1_\epsilon \neq 0$. Since $\tilde{R}_\zeta = 0$ above this edge and since $\tilde{R}_\xi$ vanishes at $\theta = 0, \pi$, we obtain two segments which are strongly coupled loci in IIA string theory. The $(\theta, \xi)$-fiber over the given edge is a squashed two-sphere, which reduces to a vertical segment above the edge's endpoints, unless one of the endpoints lies at $\eta = 0$, in which case the fiber does not degenerate there. These two cases are shown in the upper figures. The horizontal segments result by fibering the north and south poles of the $(\theta, \xi)$-fiber over the edge. The lower figure shows the coordinates along a generic $(\theta, \xi)$ fiber.

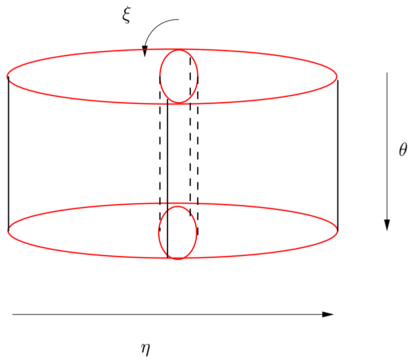


**Figure 9:** Schematic depiction of the horizontal branes sitting above the edge $c$ of $\Delta_M$ for the case $\nu^1_\epsilon = 0$. The locus $\rho = 0$ at a fixed value of $r$ is a 3-dimensional cylinder whose cross section is a two-sphere spanned by $\eta$ and $\xi$. The internal directions of each 6-brane comprise $r$ and one of the horizontal two-spheres which bound this cylinder. The figure also shows a cross section of the three-dimensional cylinder at a fixed value of $\eta$. This cross section is a two-dimensional cylinder with coordinates $\theta$ and $\xi$, the degeneration of the $(\theta, \xi)$-fiber above the locus $\rho = 0$.

Since $T = 0$, equation (4.57) reduces to:

$$C = \frac{1}{\eta} d\xi + \frac{L_1 \cos\zeta}{\eta \tan\theta} d\rho + L_1 d\zeta + O(\rho)\,, \tag{4.65}$$

so that $C_\rho$ blows up for $\rho = 0$ and $\theta = 0, \pi$ while $C_\xi$ and $C_\zeta$ remain finite. Relation (4.58) gives:

$$\int_{\Gamma_\zeta} C = 2\pi L_1 = 2\pi \nu^2_\epsilon\,. \tag{4.66}$$

In this relation, we integrate along the circle $\Gamma_\zeta$ obtained by fixing $\theta = 0$ or $\pi$ as well as $r, \xi$ and $\eta$, and a small (but non-vanishing) value of $\rho$. Equation (4.66) indicates the presence of RR flux through the 2-dimensional disk $D_\zeta$ bounded by $\Gamma_\zeta$:

$$\int_{D_\zeta} F_2 = 2\pi\nu_\epsilon^2 \,, \tag{4.67}$$

where $F_2 := dC$. Since the radius of such a $\zeta$-circle can be made arbitrarily small, this equation indicates the presence of a source. The flux sources must be localized at $\theta = 0$ and $\theta = \pi$ since $C_\rho$ becomes singular there.

This establishes the presence of two $D6$-branes (of multiplicity $|\nu_\epsilon^2|$) at $\theta = 0, \pi$. Their internal directions span $r$, $\eta$ and $\xi$, which for $r_0 = 0$ are the cones over the two-spheres bounding the cylinder in figure 9. In this case, the full worldvolume of each such brane is topologically a copy of $\mathbb{R}^7$ spanned by the external $\mathbf{E}^{3,1}$ coordinates and the internal directions mentioned above. Vanishing of $T = \nu_\epsilon^1$ implies that $|\nu_\epsilon^2| = gcd(0, \nu_\epsilon^2) = gcd(\nu_\epsilon^1, \nu_\epsilon^2)$ coincides with the integer $m_e = m_{-e}$ introduced in [16] and reviewed in subsection 2.2 ($e$ is one of the two edges of $\Delta$ lying above the given edge of $\Delta_M$). Therefore, the D6-branes sitting at $\theta = 0$ and $\theta = \pi$ have multiplicity $|m_e|$, and carry an SU($|m_e|$) gauge theory on their worldvolume. This agrees with our expectations and with the conclusions of [16]. Since we divided by the isometry associated with $\phi$, we find D6-branes corresponding to those singular loci of $Y_H$ which are fixed by this isometry – these are the horizontal loci for which $T = \nu_\epsilon^1 = 0$.

### 4.4 Behavior on the vertical locus

Recall from section 3 that on the vertical locus one has $\rho = 0$ and $\eta = \eta_j := -\nu_j^1/\nu_j^2$ for some $j$. Thus $L_2 = |\nu_j^2|/(|\eta - \eta_j|) + O(\eta - \eta_j)$ tends to infinity on this locus. Then equations (4.36) give:

$$U_{11} = \frac{f\eta_j^2}{2L_0^2}\sin^2(\theta)\,, \qquad U_{22} = \frac{f}{2L_0^2}\sin^2(\theta)\,, \qquad U_{12} = \frac{f\eta_j}{2L_0^2}\sin^2(\theta)\,, \tag{4.68}$$

while the determinant of $U$ vanishes. Equation (4.54) gives:

$$g_A^{4/3} = \frac{r^2 f\eta_j^2}{4L_0^2}\sin^2(\theta) + O(\rho)\,. \tag{4.69}$$

The behavior of $C$ results by taking the limit $\eta \to \eta_j$ in equations (4.57). Let us fix some $j = 1 \ldots n$ and concentrate on the piece of the vertical locus lying above the vertex $P_j$ of $\Delta_M$ given by $\rho = 0$ and $\eta = \eta_j$. Once again, we have two possibilities:

(a) $\eta_j \neq 0 \Leftrightarrow \nu_j^1 \neq 0$. In this case $g_A$ has a non-vanishing limit for $\rho \to 0$ and the loci $\theta = 0, \pi$ are strongly coupled. Equation (4.52) shows that that the $(\theta, \xi)$-fiber degenerates to a segment of (relative) length $(\pi r/2)\sqrt{f}$.

Equation (4.57) gives:

$$C = \frac{1}{\eta_j}d\xi + \frac{L_1\cos\zeta}{\eta_j\tan\theta}d\rho + L_1 d\zeta + O(\rho)\,. \tag{4.70}$$

(b) $\eta_j = 0 \Leftrightarrow \nu_j^1 = 0$. In this case the coupling constant $g_A$ vanishes on the fiber $S_j^2(\theta, \xi)$ sitting above $\rho = \eta = 0$, which carries the metric (4.53). The behavior of the RR one-form is more subtle than before, because (4.57) contains the combination $\eta L_2$. To find its limit for $\eta \to 0$, notice that $\epsilon_k(0) = \mathrm{sign}(\nu_k^1)$ for $k \neq j$ and $\epsilon_j(\eta) = \mathrm{sign}(\eta)\,\mathrm{sign}(\nu_j^2)$. The limit of the latter depends on whether $\eta$ approaches zero from below or from above. If we let $\kappa = \mathrm{sign}(\eta)$, then the two directional limits correspond to $\kappa = +1$ and $\kappa = -1$ respectively. Since $\nu_j^1$ vanishes, we have $L_0(0) = \sum_{k\neq j} |\nu_k^1|$ and $T(0) = \sum_{k\neq j} \epsilon_k(0)\nu_k^1 = \sum_{k\neq j} \mathrm{sign}(\nu_k^1)\nu_k^1 = \sum_{k\neq j} |\nu_k^1| = L_0(0)$. Upon defining the vector $\tilde{\nu}_j := \sum_{k\neq j} \epsilon_k \nu_k = \sum_{k\neq j} \mathrm{sign}(\nu_k^1)\nu_k$, we obtain:

$$L_0(0) = T(0) = \tilde{\nu}_j^1 \,. \tag{4.71}$$

Notice that $T(\eta)$ equals $T(0)$ on an entire vicinity of $\eta = 0$ (this follows using the fact that $T(0)$ is a locally constant function). On the other hand, we have $L_1 = \epsilon_j \nu_j^2 + \sum_{k\neq j} \epsilon_k \nu_k^2$, so that:

$$\lim_{\substack{\eta\to 0 \\ \mathrm{sign}(\eta)=\kappa}} L_1(\eta) = \kappa|\nu_j^2| + \tilde{\nu}_j^2 \,. \tag{4.72}$$

The quantity $L_2(\eta) = \sum_{k=1}^n \frac{(\nu_k^2)^2}{|\nu_k^2\eta + \nu_k^1|}$ has the following behavior for $\eta \to 0$:

$$L_2(\eta) = \kappa\frac{|\nu_j^2|}{\eta} + \sum_{k\neq j} \frac{(\nu_k^2)^2}{|\nu_k^1|} + O(\eta) \,. \tag{4.73}$$

This implies:

$$\lim_{\substack{\eta\to 0 \\ \mathrm{sign}(\eta)=\kappa}} \eta L_2 = \kappa|\nu_j^2| \,. \tag{4.74}$$

Using (4.57), we obtain:

$$\begin{aligned}
C_\xi^{(\kappa)} &:= \lim_{\substack{\eta\to 0 \\ \mathrm{sign}(\eta)=\kappa}} C_\xi = -\kappa|\nu_j^2|\frac{1-(f/2)\sin^2(\theta)}{\tilde{\nu}_j^1} - \frac{\tilde{\nu}_j^2}{\tilde{\nu}_j^1} \\
C_\rho^{(\kappa)} &:= \lim_{\substack{\eta\to 0 \\ \mathrm{sign}(\eta)=\kappa}} C_\rho = \left(\frac{f}{2}\frac{(\nu_j^2)^2}{\tilde{\nu}_j^1} + \kappa|\nu_j^2|\frac{f}{2}\frac{\tilde{\nu}^2}{\tilde{\nu}^1}\right)\sin(\theta)\cos(\theta)\cos(\zeta) \\
C_\zeta^{(\kappa)} &:= \lim_{\substack{\eta\to 0 \\ \mathrm{sign}(\eta)=\kappa}} C_\zeta = \tilde{\nu}_j^2 + \kappa|\nu_j^2| \,.
\end{aligned} \tag{4.75}$$

These expressions show that $C$ is discontinuous along the vertical locus $\eta = \eta_j = 0$. The discontinuity jumps of $C_\xi$ and $C_\zeta$ are given by:

$$\begin{aligned}
(\Delta C)_\xi &:= \lim_{\substack{\eta\to 0 \\ \eta>0}} C_\xi - \lim_{\substack{\eta\to 0 \\ \eta<0}} C_\xi = -2\frac{|\nu_j^2|}{\tilde{\nu}_j^1}\left[1 - \frac{f}{2}\sin^2(\theta)\right], \\
(\Delta C)_\zeta &:= \lim_{\substack{\eta\to 0 \\ \eta>0}} C_\zeta - \lim_{\substack{\eta\to 0 \\ \eta<0}} C_\zeta = 2|\nu_j^2| \,.
\end{aligned} \tag{4.76}$$

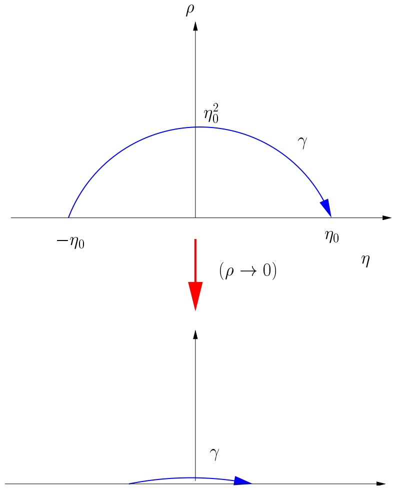


**Figure 10:** The curve $\gamma$. The parameter $\eta_0$ is taken to be of order $\rho$ (for example, $\eta_0 = \rho$). As $\rho$ tends to zero, the point $\eta_0^2$ approaches zero faster than $\eta_0$. As a consequence, the curve $\gamma$ looks like an infinitesimally small segment along the $\eta$-axis in this limit.

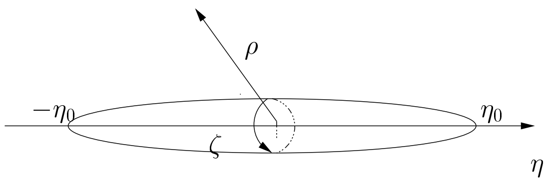


**Figure 11:** The two-sphere $\Sigma$ determined by $\gamma$ in the directions transverse to the worldvolume. The internal worldvolume coordinates $r, \theta$ and $\xi$ are fixed to some arbitrary values. As $\rho$ tends to zero, the $\zeta$-circle collapses faster than $\eta_0$. The point $(r, \theta, \xi)$ of the internal worldvolume sits at $\eta_0 = \rho = 0$.

Since the IIA coupling vanishes on $S_j^2(\theta, \xi)$, we expect a 6-brane whose worldvolume comprises $\mathbf{E}^{3,1}$ and the cone over $S_j^2$. To confirm this picture, we shall compute the 'magnetic' RR flux produced by our brane.

The charge computation requires us to fix the internal worldvolume coordinates $r, \theta, \xi$ to some values and find a closed surface sitting in the transverse directions $\rho, \eta, \zeta$ and surrounding the worldvolume point $(r, \theta, \xi)$. For this, consider the curve $\gamma$ given by the following equation in coordinates $(\rho, \eta)$:

$$\rho = \eta_0^2 - \eta^2 \, . \tag{4.77}$$

Here $\eta_0$ is a fixed parameter. Since we wish to use the asymptotic expressions determined above (which are valid only to leading order in $\rho$), we will take $\eta_0$ to be very small, so that the curve sits in a small vicinity of $\rho = \eta = 0$ (figure 10 ). Inclusion of the remaining transverse coordinate (namely $\zeta$) gives an $S^1$ fibration over this curve, whose fiber collapses to a point above the endpoints $\rho = 0, \eta = \pm\eta_0$. This gives a surface $\Sigma$ (topologically a two-sphere) which surrounds the worldvolume point $(r, \theta, \xi)$ sitting at $\rho = \eta = 0$ (figure 11).

The magnetic flux of $F_2 = dC$ through $\Sigma$ is given by the integral $\Phi = \int_\Sigma F_2$. To compute this, one should in principle start with relation (4.57) and perform the integral of

$dC$ over $\Sigma$, while keeping in mind that $\eta_0$ is taken to be very small. It is easy to find the result without performing the entire computation. For this, notice that the integral only receives contributions from the components $F_{\zeta\eta}$ and $F_{\zeta\rho}$ (the second is relevant because $d\rho$ and $d\eta$ are related on the surface $\Sigma$, which is also why $F_{\rho\eta}$ gives zero contribution). Using the defining equation of $\gamma$, one finds $d\rho = -2\eta d\eta$ on $\Sigma$, which means that, after pull-back to this surface, the component $F_{\zeta\rho}$ will be multiplied by $\eta$. Since $\eta$ runs between $-\eta_0$ and $\eta_0$ and since $\eta_0$ is taken to zero in the end, this component does not contribute to the final result. Therefore, it suffices to consider the contribution coming from $F_{\zeta\eta}$, which gives:

$$\Phi = \int_\Sigma F_{\zeta\eta} d\zeta \wedge d\eta = \int d\zeta \int_{-\eta_0}^{\eta_0} d\eta \frac{\partial C_\zeta}{\partial \eta} = \int d\zeta [C_\zeta(\eta_0) - C_\zeta(-\eta_0)] . \tag{4.78}$$

Taking the limit $\eta_0 \to 0$, the integrand reduces to $(\Delta C)_\zeta = C_\zeta^{(+)} - C_\zeta^{(-)}$, so that:

$$\Phi = \int_0^{2\pi} d\zeta (\Delta C)_\zeta . \tag{4.79}$$

Using the last of equations (4.76), we find:

$$\Phi = 4\pi |\nu_j^2| . \tag{4.80}$$

As for the horizontal locus, we find agreement with our expectations and with the results of [16]: one obtains localized D6-branes for a vertical locus which satisfies $\nu_j^1 = 0$ and thus is fixed under the action of $\mathrm{U}(1)_\phi$.

**Observation.** If one takes into account the possibility of further $\mathbb{Z}_2$ identifications above certain edges or vertices of $\Delta_M$ (see observation 3 in subsection 3), then the reduction to IIA will produce an identification $\zeta \equiv \zeta + \pi$ on such a locus. In this case, the range of integration in relations (4.66) and (4.79) must be restricted to $[0, \pi]$, which means that the result in the right hand side of these relations must be divided by two. This agrees with the results of [16], which show that the gauge group content may be half of that predicted by (4.66) and (4.79) in certain situations. Precise criteria for deciding when this happens can be found in [16].

## 5. T-dual IIB description

### 5.1 The type IIB solution

The metric (4.19) is still invariant under shifts of the coordinate $\psi$. In this section we will T-dualize along the direction of this coordinate. Applying the Buscher rules [47, 48] we obtain the following IIB fields in the string frame for the NS-NS sector:

$$\begin{aligned}
\varphi_B &= \ln U_{11} - \frac{1}{2} \ln \det U \\
B^{NS} &= g^{(A)}_{\psi m} g^{(A)-1}_{\psi\psi} d\psi \wedge dx^m \\
ds^2_{(B)} &= \left[ g^{(A)}_{mn} - g^{(A)-1}_{\psi\psi} g^{(A)}_{\psi m} g^{(A)}_{\psi n} \right] dx^m dx^n + g^{(A)-1}_{\psi\psi} d\psi^2 .
\end{aligned} \tag{5.1}$$

Here $x^m$ denote the 9 coordinates different from $\psi$. Since the IIA background contains no $B$-field, the T-duality rules mapping it to IIB are simpler than the general ones.

In the R-R sector, we obtain:

$$\begin{aligned} l &= C_\psi = \frac{U_{12}}{U_{11}} \\ B^R &= \left[C_m - g^{(A)-1}_{\psi\psi}\, g^{(A)}_{\psi m}\, C_\psi\right] dx^m \wedge d\psi\,, \end{aligned} \tag{5.2}$$

where $l$ is the axion and $B^R$ the RR 2-form. The IIB background does not contain a RR 3-form, because of the vanishing $B$-field in the IIA solution.

We remind the reader that the relation between string and Einstein frames is:

$$ds^2_E = e^{-1/2\varphi}\, ds^2_S\,. \tag{5.3}$$

As in the previous section, it will be convenient to use the 'relative' type IIB metric $\tilde{g}^{(B)}_{ij}$, related to $g^{(B)}_{ij}$ through:

$$g^{(B)}_{ij} = \left(\frac{r^2 U_{11}}{2}\right)^{1/2} \tilde{g}^{(B)}_{ij}\,. \tag{5.4}$$

The IIB coupling results from relation (5.1):

$$g_B = e^{\varphi_B} = \frac{U_{11}}{\sqrt{\det U}}\,. \tag{5.5}$$

Hence the axion-dilaton modulus is $\tau = l + (i/g_B) = (U_{12} + i\sqrt{\det U})/(U_{11})$. Recall that IIB string theory has a non-perturbative duality symmetry which acts on $\tau$ and on the two-form fields through:

$$\tau \to \frac{a\tau + b}{c\tau + d}\,, \qquad \mathcal{B} \to S^{-T}\mathcal{B}\,, \tag{5.6}$$

where $S = \begin{bmatrix} a & b \\ c & d \end{bmatrix}$ is an SL$(2, \mathbb{Z})$ matrix and $\mathcal{B} = \begin{bmatrix} B^{NS} \\ B^R \end{bmatrix}$.

### 5.2 Behavior of the IIB solution for $\rho \to 0$

We are now ready to study the behavior of the type IIB solution near the positions of the horizontal and vertical loci. We once again start by extracting the asymptotics of various fields in the limit $\rho \to 0$.

#### 5.2.1 Asymptotics for the metric induced in the $\theta, \chi, \psi$ directions

Using relations (5.1) and (4.40), we compute:

$$\begin{aligned} \tilde{g}^{(B)}_{\psi\psi} &= \frac{2\eta^2\delta}{r^2} + \frac{4}{r^2 f}\frac{T^2}{\sin^2(\theta)} + O(\rho) \\ \tilde{g}^{(B)}_{\theta\theta} &= \tilde{g}^{(A)}_{\theta\theta} = \frac{r^2 f}{4} + O(\rho^2) \\ \tilde{g}^{(B)}_{\theta\chi} &= O(\rho) \\ \tilde{g}^{(B)}_{\chi\chi} &= O(\rho)\,, \\ \tilde{g}^{(B)}_{\psi\chi} &= \tilde{g}^{(B)}_{\psi\theta} = 0\,. \end{aligned} \tag{5.7}$$

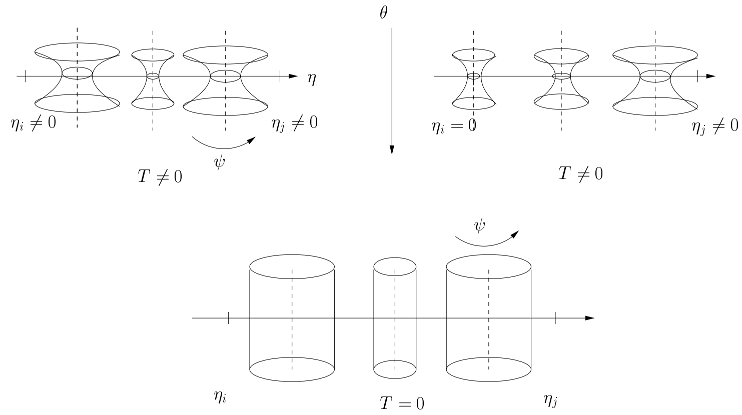


**Figure 12:** The IIB $(\theta, \psi)$-fibers above various edges of $\Delta_M$.

Note that the $\chi$-circle is always collapsed to a point for $\rho = 0$. We have:

$$d\tilde{s}_B^2|_{\theta,\chi,\psi} = \frac{r^2 f}{4} d\theta^2 + \frac{2}{r^2 f} \frac{2T^2 + f\eta^2\delta\sin^2(\theta)}{\sin^2(\theta)} d\psi^2 + O(\rho)\,, \tag{5.8}$$

which shows that the locus $\rho = 0$ has codimension two. In particular, the $\theta$-fiber degenerates to a segment of (relative) length $\pi r\sqrt{f}/2$ above the entire boundary of the hyperbolic plane. The $\psi$-circle fibers over this segment with the radius given by (5.8), while the $\chi$-circle is collapsed to zero size. Above an edge having $T = 0$, (5.8) reduces to:

$$d\tilde{s}_B^2|_{\theta,\chi,\psi} = \frac{r^2 f}{4} d\theta^2 + \frac{2\eta^2\delta}{r^2} d\psi^2 + O(\rho)\,, \tag{5.9}$$

which shows that the $(\theta, \chi, \psi)$-fibers are cylinders of squared relative radius $2\eta^2\delta/r^2$; this radius tends to infinity at the two endpoints of the given edge of $\Delta_M$ (none of which can correspond to $\eta = 0$). Above an edge with $T \neq 0$, the squared $\psi$-circle radius varies with $\theta$ and is symmetric under $\theta \to \pi - \theta$. For fixed $\eta$, it tends to an infinite value for $\theta = 0, \pi$ and reaches its minimum $2(f\eta^2\delta + 2T^2)/r^2 f$ for $\theta = \pi/2$. This squared radius tends to infinity for any $\theta$ at a vertex $\eta_j \neq 0$, and reduces to $4T^2/(r^2 f \sin^2(\theta))$ for $\eta = 0$. The situation is summarized in figure 12.

#### 5.2.2 Asymptotic behavior of the modular parameter and NS-NS/RR two-forms

The modular parameter has the following asymptotics for $\rho \to 0$:

$$\begin{aligned} \operatorname{Re}\tau &= \frac{-2L_1 T + f\eta\delta\sin^2(\theta)}{2T^2 + f\eta^2\delta\sin^2(\theta)} + O(\rho) \\ \operatorname{Im}\tau &= \frac{L_0\sqrt{2f\delta}\sin(\theta)}{2T^2 + f\eta^2\delta\sin^2(\theta)} + O(\rho)\,. \end{aligned} \tag{5.10}$$

For the NS-NS and R-R two-forms, one obtains:

$$\mathcal{B}_{\psi\rho} = \nu_\epsilon \frac{L_1}{L_0} \frac{\cos\chi}{\tan\theta} + O(\rho)$$

$$\begin{aligned}
\mathcal{B}_{\psi\eta} &= O(\rho) \\
\mathcal{B}_{\psi u^1} &= -\nu_\epsilon \frac{\sin\chi}{\sin\theta} + O(\rho) \\
\mathcal{B}_{\psi u^2} &= \nu_\epsilon \frac{\cos\chi}{\sin\theta} + O(\rho)\,,
\end{aligned} \tag{5.11}$$

where we used $T = \nu_\epsilon^1$ and $L_1 = \nu_\epsilon^2$. Converting to the coordinates $(\rho, \eta, \psi, \theta, \chi)$, we obtain:

$$\mathcal{B} = \nu_\epsilon \left[ \frac{L_1}{L_0} \frac{\cos\chi}{\tan\theta} d\psi \wedge d\rho + d\psi \wedge d\chi \right] + O(\rho)\,. \tag{5.12}$$

Integration over a $(\chi, \psi)$-torus $\Gamma_{\chi,\psi}$ at a small but non-vanishing $\rho$ gives $\nu_\epsilon^1$ units of NS-NS flux and $\nu_\epsilon^2$ units of R-R flux through the 3-dimensional volume $S_{\chi,\psi}$ with boundary $\Gamma_{\chi,\psi}$:

$$\int_{S_{\chi,\psi}} d\mathcal{B} = \int_{\Gamma_{\chi,\psi}} \mathcal{B} = (2\pi)^2 \nu_\epsilon\,. \tag{5.13}$$

As in [16], we write $\nu_\epsilon = m_\epsilon t_\epsilon$, where $m_\epsilon = gcd(\nu_\epsilon^1, \nu_\epsilon^2)$ and $t_\epsilon$ is a primitive integral vector. Since $t_\epsilon^1$ and $t_\epsilon^2$ are coprime integers, there exist coprime integers $a$ and $b$ such that $at_\epsilon^2 - bt_\epsilon^1 = 1$. Then the matrix $S = \begin{bmatrix} a & b \\ t_\epsilon^1 & t_\epsilon^2 \end{bmatrix}$ belongs to $\mathrm{SL}(2, \mathbb{Z})$ and has the property:

$$S^{-T} \nu_\epsilon = \begin{bmatrix} 0 \\ m_\epsilon \end{bmatrix}. \tag{5.14}$$

Using this transformation in (5.6) allows us to bring $B^{NS}$ and $B^R$ to the forms:

$$B'^{NS} = O(\rho) \tag{5.15}$$

and

$$B'^{R} = m_\epsilon \left[ \frac{L_1}{L_0} \frac{\cos\chi}{\tan\theta} d\psi \wedge d\rho + d\psi \wedge d\chi \right] + O(\rho)\,. \tag{5.16}$$

After this transformation, the modular parameter (5.10) becomes:

$$\tau' = \frac{a\,[-2L_1 T + (f\eta\delta + iL_0\sqrt{2f\delta}) \sin^2(\theta)] + b\,[2T^2 + f\eta^2\delta\sin^2(\theta)]}{t_\epsilon^1\,[-2L_1 T + (f\eta\delta + iL_0\sqrt{2f\delta}) \sin^2(\theta)] + t_\epsilon^2\,[2T^2 + f\eta^2\delta\sin^2(\theta)]} + O(\rho)\,. \tag{5.17}$$

### 5.3 Behavior on the horizontal locus

Recall that the horizontal locus is obtained for $\rho = 0$ and $\theta = 0, \pi$. Fixing an edge of $\Delta_M$, we distinguish two situations:

**(a)** $T \neq 0 \Leftrightarrow \nu_\epsilon^1 \neq 0$. In this case, the radius of the $\psi$-circle blows up at $\theta = 0, \pi$ and reaches its minimum for $\theta = \pi/2$. Equation (5.10) gives:

$$\mathrm{Re}(\tau) = -\frac{L_1}{T} + O(\rho) = -\frac{\nu_\epsilon^2}{\nu_\epsilon^1} + O(\rho)\,, \quad \mathrm{Im}(\tau) = O(\rho) \quad \text{for} \quad \theta = 0, \pi\,. \tag{5.18}$$

In particular, the IIB coupling constant $g_B$ tends to infinity, while the axion reaches a finite value. Equation (5.13) shows [16] the presence of NS5 and D5-brane charge on this locus. Due to symmetry of the asymptotic solution with respect to shifts of $\psi$, the worldvolume directions are spanned by $\mathbf{E}^{3,1}$ together with $r, \eta$ and $\psi$, which means that the 5-branes are *delocalized* in the direction $\psi$.

**(b)** $T = 0 \Leftrightarrow \nu_\epsilon^1 = 0$. In this case (5.7) gives:

$$\tilde{g}_{\psi\psi}^{(B)} = \frac{2\eta^2}{r^2}\delta + O(\rho)\,, \tag{5.19}$$

so that the (relative) radius of the $\psi$-circle remains finite. Relations (5.10) give:

$$\mathrm{Re}\,\tau = \frac{1}{\eta} + O(\rho)\,, \qquad \mathrm{Im}\,\tau = \frac{L_0}{\eta^2 \sin\theta}\sqrt{\frac{2}{f\delta}} + O(\rho)\,. \tag{5.20}$$

In particular, the IIB coupling constant vanishes for $\rho = 0$ and $\theta = 0, \pi$, so that the horizontal locus is weakly coupled. Since $T = 0$, one has $L_0 = \eta L_1$, and equation (5.12) becomes:

$$\mathcal{B} = \nu_\epsilon\left[\frac{1}{\eta}\frac{\cos\chi}{\tan\theta}d\psi\wedge d\rho + d\psi\wedge d\chi\right] + O(\rho)\,. \tag{5.21}$$

Equation (5.13) gives:

$$\int_{S_{\chi,\psi}} dB^{NS} = 0\,, \qquad \int_{S_{\chi,\psi}} dB^R = (2\pi)^2\nu_\epsilon^2\,. \tag{5.22}$$

This shows that the horizontal locus contains a $D5$-brane of multiplicity $|\nu_\epsilon^2| = m_\epsilon = gcd(0, \nu_\epsilon^2)$. The worldvolume directions are $\mathbf{E}^{3,1}$ and $r, \eta, \psi$, which shows that the D5-brane is *delocalized along* $\psi$. Since the T-dual horizontal 6-brane is localized for $T = 0$, this delocalization is standard: one has performed a T-duality along the direction $\psi$ which lies along the worldvolume of the IIA D6-brane.[17]

### 5.4 Behavior on the vertical locus

Let us consider the vertical locus $\rho = 0, \eta \to \eta_j := -\nu_j^1/\nu_j^2$. Once again, we distinguish two situations:

[16] One may wonder whether the flux computation of (5.13) can be applied to the current situation in which $\psi$ is a worldvolume coordinate. Since a delocalized 5-brane can be viewed as $N$ localized 5-branes at positions $\psi_0, \psi_0 + 2\pi/N, \ldots, \psi_0 + (N-1)2\pi/N$ along the $\psi$-circle in the limit $N \to \infty$, in the calculation of the 5-brane flux we can view the $\psi$ direction as transverse rather than longitudinal direction. We will use this point of view again in the remainder of this section.

[17] From the worldsheet perspective, delocalization appears due to the fact that the von Neumann conditions $\partial_n X^i = 0$ (where $X^i$ are the transverse coordinates) are purely differential, while the Dirichlet conditions contain a differential part $\partial_\tau X^i = 0$ and an 'integral' part $X^i_{CM} = a^i$ (where $X^i_{CM}$ are the string center of mass coordinates and $a^i$ characterize the position of the D-brane in the transverse directions). In a general background, T-duality translates the von Neumann conditions into the differential part of the Dirichlet conditions, which fixes the boundary behavior of the oscillator modes but not that of the center of mass mode. Except for particular backgrounds, the condition $X^i_{CM} = a^i$ cannot be recovered by this process, which means that the dual D-brane can become delocalized (i.e. $a^i$ can take arbitrary values).



JHEP10(2002)038

**(a)** $\eta_j \neq 0 \Leftrightarrow \nu_j^1 \neq 0$. In this case, equation (5.7) shows that the (relative) radius of the $\psi$ circle tends to infinity for $\eta \to \eta_j$. Relation (5.10) gives:

$$\mathrm{Re}\,\tau = \frac{1}{\eta_j} = -\frac{\nu_j^2}{\nu_j^1}\,, \quad \mathrm{Im}\,\tau = 0\,. \tag{5.23}$$

The second equation shows that the IIB coupling constant tends to infinity. Therefore, this locus does not admit a perturbative interpretation in IIB string theory.

**(b)** $\eta_j = 0 \Leftrightarrow \nu_j^1 = 0$. In this case, we showed in subsection 4.4 that $L_0(0) = T(0) = \tilde{\nu}_j^1$ and $\lim_{\eta\to 0} L_1 = \kappa|\nu_j^2| + \tilde{\nu}_j^2$, where $\kappa = \mathrm{sign}(\eta)$ and $\eta \to 0$ is a directional limit. Using the fact that $\eta L_2$ tends to $\kappa|\nu_j^2|$, equation (5.7) gives:

$$\tilde{g}^{(B)}_{\psi\psi} = \frac{4}{r^2 f}\frac{(\tilde{\nu}_j^1)^2}{\sin^2(\theta)} + O(\rho)\,, \tag{5.24}$$

so that the radius of the $\psi$-circle is finite for $\theta \neq 0, \pi$. Relations (5.10) imply:

$$l = Re\tau = -\frac{\tilde{\nu}_j^2}{\tilde{\nu}_j^2} - \kappa\frac{|\nu_j^2|}{\tilde{\nu}_j^1}(1 - \frac{f}{2}\sin^2\theta) + O(\rho)\,, \qquad |Im\tau| = \infty\,. \tag{5.25}$$

Finally, equation (5.12) gives:

$$\begin{aligned} B^{NS}_{\psi\rho} &= [\tilde{\nu}_j^2 + \kappa|\nu_j^2|]\,\frac{\cos\chi}{\tan\theta} + O(\rho)\,, & B^{R}_{\psi\rho} &= \left[\frac{(\nu_j^2)^2 + (\tilde{\nu}_j^2)^2}{\tilde{\nu}_j^1} + \kappa|\nu_j^2|\frac{2\tilde{\nu}_j^2}{\tilde{\nu}_j^1}\right]\frac{\cos\chi}{\tan\theta} + O(\rho) \\ B^{NS}_{\psi\chi} &= \tilde{\nu}_j^1 + O(\rho)\,, & B^{R}_{\psi\chi} &= \tilde{\nu}_j^2 + \kappa|\nu_j^2| + O(\rho)\,. \end{aligned} \tag{5.26}$$

It may seem that the vertical locus supports a weakly-coupled D7-brane whose world-volume is spanned by the directions of $\mathbf{E}^{3,1}$ and $r, \theta, \chi, \psi$. However recall from (5.8) that the $\chi$-circle is shrunk to a point for $\rho \to 0$. Hence we don't have enough dimensions for a D7-brane, and we must interpret this 7- dimensional world-volume as a *delocalized D5-brane* (the delocalization is along the $\psi$-direction).

To substantiate this interpretation, let us consider the same curve $\gamma$ as in section 4.4 (figure 10). Since the $\chi$-circle collapses for $\rho = 0$, fibering it over $\gamma$ at a small but nonzero value of $\rho$ gives a surface $\Sigma$ similar to that of figure 11 (see figure 13 below). We have transverse coordinates $\rho, \eta$ and $\chi$, together with the delocalization direction $\psi$ which we view as 'transverse' as explained above. We shall compute the flux of the 3-form $F_3 = d\mathcal{B}$ through a three-dimensional body $\Sigma'$ cutting the directions $\rho, \eta, \chi$ *and* $\psi$ and surrounding a point sitting at $\rho = \eta = 0$ and at some fixed values of $r$ and $\theta$. For this, we choose the three-dimensional space $\Sigma'$ to be given by the $\psi$-circle fibration above $\Sigma$ (see figure 13).

An argument similar to that of section 4.4 shows that the flux of $F_3 = d\mathcal{B}$ through $\Sigma'$ receives contributions only from the component $F_{\eta\psi\chi}$ (the contribution from the pull-back of $F_{\rho\chi\psi}$ vanishes since $\eta$ is very small and $d\rho = -2\eta d\eta$ on $\Sigma'$). Equation (5.12) shows that $F_{\eta\psi\chi} = \frac{\partial\mathcal{B}_{\psi\chi}}{\partial\eta}$ (to first order in $\rho$), so that the flux of interest is given by:

$$\Phi = \begin{bmatrix}\Phi^{NS}\\ \Phi^{R}\end{bmatrix} = \int_{\Sigma'} d\mathcal{B} = \int d\chi \int d\psi (\Delta\mathcal{B})_{\psi\chi} = \begin{bmatrix}0\\ 2(2\pi)^2|\nu_j^2|\end{bmatrix}. \tag{5.27}$$

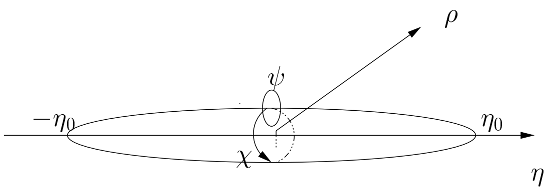


**Figure 13:** The 3-dimensional space $\Sigma'$ and the surface $\Sigma$ for type IIB vertical branes. The $\psi$-circle is fibered over the surface $\Sigma$ shown in the figure (this fibration gives $\Sigma'$).

To arrive at the last equation, we took the limit $\eta_0 \to 0$ and used relations (5.26). Notice that $(\Delta B^{NS})_{\psi\chi} = 0$, which is why we obtain only a Ramond-Ramond flux:

$$\Phi^{NS} = 0\,, \qquad \Phi^R = 2(2\pi)^2|\nu_j^2|\,. \tag{5.28}$$

Once again, we obtain agreement with the interpretation proposed in [16]: when the isometry used for performing the IIA reduction fixes the vertical locus of interest in the twistor space, then the T-dual, IIB description contains a delocalized D5-brane along the associated type II locus. As discussed there, the gauge content predicted by (5.22) and (5.28) must be 'halved' in certain situations. As in section 4, this can be understood as a consequence of possible identifications $\psi \to \psi + \pi$ above certain edges and vertices of $\Delta_M$.

**Observation.** Integrating the field strength $F_1 = dl$ over the curve $\gamma$, one obtains:

$$\int_\gamma dl = l(\eta_0) - l(-\eta_0) = \Delta l\,, \tag{5.29}$$

where $\Delta l = l(\eta = 0^+) - l(\eta = 0^-)$ is the discontinuity jump of $l$ at $\eta = 0$. From equation (5.25), we have:

$$\Delta l = -\frac{2|\nu_j^2|}{\tilde{\nu}_j^1}\left[1 - \frac{f}{2}\sin^2(\theta)\right]. \tag{5.30}$$

However, this cannot be interpreted as the presence of D7-brane charge. Indeed, such a charge must be computed by integration along a curve which surrounds a point on the D-brane worldvolume, which in our case can be obtained by considering two copies of $\gamma$ sitting at opposite angles $\chi$ and $\chi + \pi$ on the surface $\Sigma$ of figure 13. Traversing the first curve from $-\eta_0$ to $\eta_0$ and the second from $\eta_0$ to $-\eta_0$, one obtains a closed curve $\Gamma$ with the required property. The integral of $dl$ along $\Gamma$ equals $\Delta l - \Delta l = 0$, so the object of interest does not carry 7-brane charge.

## 6. The calibration 3-form

We conclude with a calculation which is somewhat aside from the rest of the paper, but may have independent applications, for example in studies of 2-dimensional $N = 1$ superconformal field theories whose targets are spaces of $G_2$ holonomy.[18] Namely we will calculate the calibration three-form. Another reason for being interested in this object is the issue

[18] This is relevant for string propagation on orbifolds of exceptional holonomy [50].

of deformed $p$-brane solutions. In [49], it is shown that one can obtain supersymmetric $p$-brane solutions supported by the Chern-Simons term in the corresponding supergravity action if one replaces the flat transverse space by a space admitting one or more covariantly constant spinors.[19] When the latter has $G_2$ holonomy, one obtains a deformed D2-brane solution in type IIA. Recall that IIA supergravity contains a RR one-form and a RR three-form. If the former vanishes, then the D2-brane solution is completely determined by a harmonic three form supported by the transverse space [49].

In [12], it is explained that the calibration 3-form has the expression:

$$\omega = h_1\omega_1 + h_2\omega_2 + h_3\omega_3\,, \tag{6.1}$$

where $h_i$ depend only on $r$ and satisfy the following conditions:

$$(h_1)' = h_2 + h_3\,, \qquad f^{-1/2}h_1 = \frac{1}{4}(r^2 f^{3/2}h_2)' = (r^2 f^{-1/2}h_3)'\,. \tag{6.2}$$

The 3-forms $\omega_i$ are determined by the connection $A^j$ on the bundle $\Lambda^{2,-}(T^*M)$, whose curvature we denote by $F^j$:

$$\omega_1 = \theta^i\wedge F^i\,, \qquad \omega_2 = dr\wedge(u^iF^i)\,, \qquad \omega_3 = dr\wedge\Sigma\,. \tag{6.3}$$

Here $\theta^i := du^i + \epsilon^{ijk}A^ju^k$ and:

$$\Sigma = \frac{1}{2}\epsilon_{ijk}u^i\theta^j\wedge\theta^k\,. \tag{6.4}$$

Using the relations (4.8) for the connection one-form, we obtain:

$$A^1 = -\frac{F_\eta}{F}d\rho + \left(\frac{1}{2\rho}+\frac{F_\rho}{F}\right)d\eta\,, \qquad A^2 = -\frac{\sqrt{\rho}}{F}d\phi\,, \qquad A^3 = \frac{\eta}{F\sqrt{\rho}}d\phi + \frac{1}{F\sqrt{\rho}}d\psi\,. \tag{6.5}$$

The curvature of this connection was calculated in [29, section 8]:[20]

$$F^1 = -\frac{F^2-4\rho^2(F_\rho^2+F_\eta^2)}{4F^2\rho^2}\,d\rho\wedge d\eta + \frac{1}{F^2}\,d\phi\wedge d\psi \tag{6.6}$$

$$\begin{aligned} F^2 &= \frac{F_\eta}{F^2\sqrt{\rho}}\,d\psi\wedge d\rho + \frac{1}{F^2\sqrt{\rho}}\left(\rho F_\rho + \eta F_\eta - \frac{F}{2}\right)d\phi\wedge d\rho - \\ &\quad - \frac{1}{F^2\sqrt{\rho}}\left(F_\rho + \frac{F}{2\rho}\right)d\psi\wedge d\eta + \frac{1}{F^2\sqrt{\rho}}\left(\rho F_\eta - \eta F_\rho - \frac{\eta}{\rho}\frac{F}{2}\right)d\phi\wedge d\eta \end{aligned} \tag{6.7}$$

$$\begin{aligned} F^3 &= -\frac{1}{F^2\sqrt{\rho}}\left(F_\rho + \frac{F}{2\rho}\right)d\psi\wedge d\rho + \frac{1}{F^2\sqrt{\rho}}\left(\rho F_\eta - \eta F_\rho - \frac{\eta}{\rho}\frac{F}{2}\right)d\phi\wedge d\rho - \\ &\quad - \frac{F_\eta}{F^2\sqrt{\rho}}\,d\psi\wedge d\eta - \frac{1}{F^2\sqrt{\rho}}\left(\rho F_\rho + \eta F_\eta - \frac{F}{2}\right)d\phi\wedge d\eta\,. \end{aligned} \tag{6.8}$$

[19] This guarantees that the deformed brane is still supersymmetric.

[20] Direct computation of the curvature of (6.5) gives (6.6) upon using the fact that the function $F(\rho,\eta)$ is not arbitrary but satisfies $F_{\rho\rho}+F_{\eta\eta} = 3F/(4\rho^2)$ [29].

It is now trivial to write down $\omega_2$. To determine $\omega_3$, we calculate the quantity $\Sigma$:

$$\Sigma = \left[\frac{F_\eta}{F}d\rho - \left(\frac{1}{2\rho} + \frac{F_\rho}{F}\right)d\eta\right] \wedge \left[\frac{(\rho u^3 + \eta u^2)}{\sqrt{\rho}F}d\phi + \frac{u^2}{\sqrt{\rho}F}d\psi - du^1\right] - \frac{u^1}{F^2}\,d\phi \wedge d\psi + \\ + \left[\frac{u^1\sqrt{\rho}}{F}(u^1du^2 - u^2du^1) + \frac{u^1\eta}{\sqrt{\rho}F}(u^3du^1 - u^1du^3) + \frac{\rho u^3 + \eta u^2}{\sqrt{\rho}F}(u^3du^2 - u^2du^3)\right] \wedge d\phi - \\ - \frac{1}{F\sqrt{\rho}}\,du^3 \wedge d\psi + \frac{1}{2}\epsilon_{ijk}u^i du^j \wedge du^k\,. \tag{6.9}$$

Using (6.8), we also compute:

$$\omega_1 = \frac{1}{F^3\sqrt{\rho}}\left\{\left(\frac{F^2}{4\rho^2} + 2F_\eta F_\rho\right)(u^3\rho + u^2\eta) - (\rho+\eta)(u^2+u^3)(F_\rho^2 + F_\eta^2) + \right. \\ \left. + \frac{F}{\rho}\left[\eta(u^2F_\eta - u^3F_\rho) - \frac{F}{\rho}(u^3\eta - u^2\rho)\right]\right\}d\phi \wedge d\rho \wedge d\eta + \\ + \frac{u^1}{\rho F^3}\,(2\rho F_\rho + \eta F_\eta)\,d\psi \wedge d\phi \wedge d\rho + \frac{1}{\sqrt{\rho}F^3} \times \\ \times \left\{u^3\left[F_\eta^2 - \left(F_\rho + \frac{F}{2\rho}\right)^2\right] + u^2\left(\frac{F^2}{4\rho^2} - (F_\rho - F_\eta)^2 + \frac{F_\eta F}{\rho}\right)\right\}d\psi \wedge d\rho \wedge d\eta + \\ + \frac{u^1}{\rho F^3}\left(2\rho F_\eta - \eta F_\rho - \frac{\eta}{\rho}\frac{F}{2}\right)d\psi \wedge d\phi \wedge d\eta + du^i \wedge F^i\,. \tag{6.10}$$

The calibration three-form is now obtained by substituting these expressions into (6.1).

## 7. Conclusions

Upon using the recent results of [29], we constructed explicit metrics for a discrete infinity of $G_2$ cones (and their one-parameter deformations) associated with toric hyperkahler cones. This allowed us to perform the type IIA reduction of the general such model, and extract its IIB dual. This leads to a large class of solutions of IIA and IIB supergravity which preserve $N = 1$ supersymmetry in the four external directions. By studying the asymptotics of the various fields in the vicinity of certain locations, we extracted the physical interpretation of such backgrounds. In particular, we showed that the resulting IIA solutions are related to systems of weakly and strongly coupled 6-branes, while their type IIB duals describe systems of localized and delocalized 5-branes. This provides an independent confirmation of the conclusions of [16].

For particular values of the discrete parameters characterizing our metrics (namely the toric hyperkahler generators $\nu_j$ of [16], which we reviewed in section 2), one can reduce through a 'good' isometry. In this case, we showed that the IIA solutions describe backgrounds containing weakly coupled D6-branes, whose type IIB duals are delocalized and weakly coupled 5-branes. A purely perturbative type II description seems to require that the associated twistor space has no isolated singularities (if such singularities are present, then the quantum dynamics of the corresponding solution could be related to certain conformal field theories in five dimensions [9], and it is unclear to us how one could describe this in type IIA at the quantum level). However, the discussion of the present paper shows the presence of D-brane charge along certain weakly coupled regions, regardless of whether the twistor space contains some isolated singularities beyond the codimension 4 singular loci responsible for the appearance of D-branes. This simply means that the somewhat mysterious CFT behaviour expected from the former is localized at the associated points in the type IIA background. Using this observation, it follows that the matter content produced by these D-branes can be identified directly from the type IIA description, although a model whose twistor space also contains isolated singularities can be expected to display further — and currently unknown — phenomena. We should perhaps also mention that explicit examples with a good isometry can be constructed through the algorithm described in [16], and some of the simplest such models (which differ from those discussed in [9]) can be found in section 8 of the reference just cited.

For models without a good isometry, the IIA reduction leads to a strongly coupled solution containing delocalized 6-branes. While our work provides a rather complete classical analysis, the quantum IIA dynamics around these backgrounds remains unknown. At least in certain limits, it is likely that a worldvolume description of our delocalized branes may involve some sort of noncommutative field theory, though a complete quantum formulation could require the full power of string field theory. We wish to stress, however, that these IIA backgrounds should be physically consistent at the quantum level, since the associated M-theory vacuum is believed to be so. The fact that the generic model in our class leads to solutions of this type underscores the relevance of exotic type II vacua whose existence is required by M-theory.

These T-dual IIA and IIB solutions form a wide generalization of systems considered in the recent work of [9], and provide a rich source of $N = 1$ type II vacua which admit an explicitly known lift to M-theory backgrounds of $G_2$ holonomy. The choices of $\nu_j$ which lead to models with a good isometry could be of interest for phenomenological applications.

## Acknowledgments

The authors thank M. Rocek for interest and encouragement. C.I.L. would like to thank the CERN Theory group for hospitality during the last stages in the preparation of this paper. The present work was supported by the Research Foundation under NSF grant PHY-0098527.

## References

[1] A. Brandhuber, *$G_2$ holonomy spaces from invariant three-forms*, *Nucl. Phys.* **B 629** (2002) 393 [hep-th/0112113].

[2] M. Cvetič, G.W. Gibbons, H. Lu and C.N. Pope, *M-theory conifolds*, *Phys. Rev. Lett.* **88** (2002) 121602 [hep-th/0112098].

[3] M. Cvetič, G.W. Gibbons, H. Lu and C.N. Pope, *A $G_2$ unification of the deformed and resolved conifolds*, *Phys. Lett.* **B 534** (2002) 172 [hep-th/0112138].

[4] A. Brandhuber, J. Gomis, S.S. Gubser and S. Gukov, *Gauge theory at large-$N$ and new $G_2$ holonomy metrics*, *Nucl. Phys.* **B 611** (2001) 179 [hep-th/0106034].

[5] S. Gukov and D. Tong, *D-brane probes of special holonomy manifolds and dynamics of $N=1$ three-dimensional gauge theories*, *J. High Energy Phys.* **04** (2002) 050 [hep-th/0202126].

[6] S. Gukov, S.-T. Yau and E. Zaslow, *Duality and fibrations on $G_2$ manifolds*, hep-th/0203217.

[7] K. Behrndt, *Singular 7-manifolds with $G_2$ holonomy and intersecting 6-branes*, *Nucl. Phys.* **B 635** (2002) 158 [hep-th/0204061].

[8] E. Witten, *Anomaly cancellation on $G_2$ manifolds*, hep-th/0108165.

[9] B. Acharya and E. Witten, *Chiral fermions from manifolds of $G_2$ holonomy*, hep-th/0109152.

[10] M. Atiyah and E. Witten, *M-theory dynamics on a manifold of $G_2$ holonomy*, hep-th/0107177.

[11] R.L. Bryant and S.M. Salamon, *On the construction of some complete metrics with exceptional holonomy*, *Duke Math. J.* **58** (1989) 829.

[12] G.W. Gibbons, D.N. Page, C.N. Pope, *Einstein metrics on $S^3$, $\mathbb{R}^3$ and $\mathbb{R}^4$ bundles*, *Commun. Math. Phys.* **127** (1990) 529.

[13] K. Galicki and H.B. Lawson Jr., *Quaternionic reduction and quaternionic orbifolds*, *Math. Ann.* **282** (1988) 1.

[14] M. Cvetič, G. Shiu and A.M. Uranga, *Chiral four-dimensional $N=1$ supersymmetric type-IIA orientifolds from intersecting d6-branes*, *Nucl. Phys.* **B 615** (2001) 3 [hep-th/0107166].

[15] M. Cvetič, G. Shiu and A.M. Uranga, *Three-family supersymmetric standard like models from intersecting brane worlds*, *Phys. Rev. Lett.* **87** (2001) 201801 [hep-th/0107143].

[16] C.I. Lazaroiu and L. Anguelova, *M-theory compactifications on certain 'toric' cones of $G_2$ holonomy*, hep-th/0204249.

[17] A. Swann, *Hyperkähler and quaternionic Kähler geometry*, *Math. Ann.* **289** (1991) 421.

[18] C.P. Boyer, K. Galicki, B.M. Mann and E.G. Rees, *Compact 3-Sasakian 7-manifolds with arbitrary second Betti number Invent. Math.* **131** (1998) 321.

[19] C. LeBrun, *Fano manifolds, contact structures, and quaternionic geometry*, *Internat. J. Math.* **6** (1995), no. 3, 419, dg-ga/9409001.

[20] C. LeBrun, *A finiteness theorem for quaternionic Kähler manifolds with positive scalar curvature*, alg-geom/9302005.

[21] C.P. Boyer and K. Galicki, *3-sasakian manifolds*, *Surveys Diff. Geom.* **7** (1999) 123 [hep-th/9810250].

[22] R. Bielawski and A.S. Dancer, *The geometry and topology of toric hyper-Kähler manifolds*, *Commun. Anal. Geom.* **8** no. 4 (2000) 727.

[23] T. Oda *Convex bodies and algebraic geometry. An introduction to the theory of toric varieties. Ergebnisse der Mathematik und ihrer Grenzgebiete* **15** Springer-Verlag, Berlin 1988.

[24] W. Fulton, *Introduction to toric varieties*, Annals of mathematics studies **131**, Princeton University Press 1993.

[25] V. Danilov, *The geometry of toric varieties*, *Russian Math. Surveys* **33** 2(1978) 97.

[26] M. Audin, *The topology of torus actions on symplectic manifolds*, *Progress in Math.* **93** Birkhauser, 1991.

[27] D.A. Cox, *The homogeneous coordinate ring of a toric variety, revised version*, *J. Algebraic Geom.* **4** (1995), no. 1, 17 [alg-geom/9210008].

[28] D.A. Cox, *Recent developments in toric geometry*, *Proc. Sympos. Pure Math.* **62**, part 2, Amer. Math. Soc., Providence 1997 [alg-geom/9606016].

[29] D.M.J. Calderbank and H. Pedersen, *Selfdual Einstein metrics with torus symmetry*, math.DG/0105263.

[30] D. Salamon, *Quaternionic-Kähler manifolds*, *Invent. Math.* **67** (1982) 143.

[31] L. Berard-Bergery, *Varietés Quaternioniennes*, unpublished lecture notes, Espalion, 1979.

[32] S. Marchiafava and G. Romani, *Sui fibrati con struttura quaternioniale generalizatta*, *Ann. Mat. Pura Appl.* **107** (1976) 131.

[33] N.J. Hitchin, A. Karlhede, U. Lindström and M. Roček, *Hyper-Kähler metrics and supersymmetry*, *Commun. Math. Phys.* **108** (1987) 535.

[34] V. Apostolov and P. Gauduchon, *Self-dual Einstein hermitian four manifolds*, math.DG/0003162.

[35] P.-Y. Casteill, E. Ivanov and G. Valent, *Quaternionic extension of the double Taub-NUT metric*, *Phys. Lett.* **B 508** (2001) 354 [hep-th/0104078].

[36] P.-Y. Casteill, E. Ivanov and G. Valent, $U(1) \times U(1)$ *quaternionic metrics from harmonic superspace*, *Nucl. Phys.* **B 627** (2002) 403 [hep-th/0110280].

[37] J.A. Wolf, *Complex homogeneous contact manifolds and quaternionic symmetric spaces*, *J. Math. Mech.* **14** (1965) 1033.

[38] D.V. Alekseevskii, *Riemannian manifolds with exceptional holonomy groups*, *Funct. Anal. Appl.* **2** (1968) 97.

[39] D.V. Alekseevskii, *Compact quaternion spaces*, *Funct. Anal. Appl.* **2** (1968) 106.

[40] B. de Wit, B. Kleijn and S. Vandoren, *Superconformal hypermultiplets*, *Nucl. Phys.* **B 568** (2000) 475 [hep-th/9909228].

[41] B. de Wit, M. Roček and S. Vandoren, *Hypermultiplets, hyper-Kähler cones and quaternion-Kähler geometry*, *J. High Energy Phys.* **02** (2001) 039 [hep-th/0101161].

[42] B. de Wit, M. Roček and S. Vandoren, *Gauging isometries on hyper-Kähler cones and quaternion-Kähler manifolds*, *Phys. Lett.* **B 511** (2001) 302 [hep-th/0104215].

[43] J.P. Gauntlett, G.W. Gibbons, G. Papadopoulos and P.K. Townsend, *Hyper-Kähler manifolds and multiply intersecting branes*, *Nucl. Phys.* **B 500** (1997) 133 [hep-th/9702202].

[44] G.W. Gibbons, *Hyperkaehler manifolds and multiply-intersecting branes*, *Nucl. Phys.* **62** *(Proc. Suppl.)* (1998) 422 [hep-th/9707232].

[45] G.W. Gibbons and P. Rychenkova, *Hyperkaehler quotient construction of BPS monopole moduli spaces*, hep-th/9608085.

[46] P.K. Townsend, *The eleven-dimensional supermembrane revisited*, *Phys. Lett.* **B 350** (1995) 184 [hep-th/9501068].

[47] T.H. Buscher, *Quantum corrections and extended supersymmetry in new sigma models*, *Phys. Lett.* **B 159** (1985) 127; *A symmetry of the string background field equations*, *Phys. Lett.* **B 194** (1987) 59; *Path integral derivation of quantum duality in nonlinear sigma models*, *Phys. Lett.* **B 201** (1988) 466.

[48] E. Bergshoeff, C.M. Hull and T. Ortin, *Duality in the type-II superstring effective action*, *Nucl. Phys.* **B 451** (1995) 547 [hep-th/9504081].

[49] M. Cvetič, H. Lu and C.N. Pope, *Brane resolution through transgression*, *Nucl. Phys.* **B 600** (2001) 103 [hep-th/0011023].

[50] S.L. Shatashvili and C. Vafa, *Superstrings and manifold of exceptional holonomy*, hep-th/9407025.

JHEP10(2002)038